Journal of Visualized Experiments

High-resolution respirometry to assess bioenergetics in cells and tissues using chamber and plate-based respirometers

--Manuscript Draft--

Article Type:	Invited Methods Collection - JoVE Produced Video
Manuscript Number:	JoVE63000R2
Full Title:	High-resolution respirometry to assess bioenergetics in cells and tissues using chamber and plate-based respirometers
Corresponding Author:	Christopher Benjamin Jackson, Ph.D, Docent University of Helsinki: Helsingin Yliopisto Helsinki, Uusimaa FINLAND
Corresponding Author's Institution:	University of Helsinki: Helsingin Yliopisto
Corresponding Author E-Mail:	christopher.jackson@helsinki.fi
Order of Authors:	Ryan Awadhpersad
	Christopher Benjamin Jackson, Ph.D, Docent
Additional Information:	
Question	**Response**
Please specify the section of the submitted manuscript.	Biology
Please indicate whether this article will be Standard Access or Open Access.	Standard Access ($1400)
Please indicate the **city, state/province, and country** where this article will be **filmed**. Please do not use abbreviations.	Helsinki / Finland
Please confirm that you have read and agree to the terms and conditions of the author license agreement that applies below:	I agree to the Author License Agreement
Please provide any comments to the journal here.	
Please confirm that you have read and agree to the terms and conditions of the video release that applies below:	I agree to the Video Release

TITLE:

High-Resolution Respirometry to Assess Bioenergetics in Cells and Tissues using Chamber and Plate-Based Respirometers

AUTHORS AND AFFILIATIONS:

Ryan Awadhpersad[1], Christopher B. Jackson*[1]

[1]Department of Biochemistry, Faculty of Medicine, University of Helsinki, Helsinki, Finland

Email addresses of authors:

Ryan Awadhpersad (ryan.awadhpersad@helsinki.fi)
Christopher B. Jackson (christopher.jackson@helsinki.fi)

*Corresponding author:

Christopher B. Jackson (christopher.jackson@helsinki.fi)

KEYWORDS:

mitochondrial bioenergetics, respiratory chain, mitochondrial disease, oxidative phosphorylation, Flux Analyzer, extracellular flux, HEK293, oxygen consumption, mitochondrial translation

SUMMARY:

Assessing oxidative phosphorylation using high-resolution respirometers has become an integral part of the functional analysis of mitochondria and cellular energy metabolism. Here, we present protocols for the analysis of cellular energy metabolism using chamber and microplate-based high-resolution respirometers and discuss the key benefits of each device.

ABSTRACT:

High-resolution respirometry (HRR) allows monitoring oxidative phosphorylation in real-time for analysis of individual cellular energy states and assessment of respiratory complexes using diversified substrate-uncoupler-inhibitor titration (SUIT) protocols. Here, the usage of two high-resolution respirometry devices is demonstrated, and a basic collection of protocols applicable for the analysis of cultured cells, skeletal and heart muscle fibers, and soft tissues such as the brain and liver are presented. Protocols for cultured cells and tissues are provided for a chamber-based respirometer and cultured cells for a microplate-based respirometer, both encompassing standard respiration protocols. For comparative purposes, CRISPR-engineered HEK293 cells deficient in mitochondrial translation causing multiple respiratory system deficiency are used with both devices to demonstrate cellular defects in respiration. Both respirometers allow for comprehensive measurement of cellular respiration with their respective technical merits and suitability dependent on the research question and model under study.

INTRODUCTION:

Mitochondria fulfill the key provision of energy and are a compartmentalized organelle contributing to essential cellular bioenergetic and metabolic processes such as anabolism of

nucleotides, lipids and amino acids, iron-sulfur cluster biogenesis and are implicated in signaling such as for controlled cell death[1–3]. Mitochondrial bioenergetics through oxidative phosphorylation contributes to almost all cellular processes within the cell, and consequently, mitochondrial dysfunctions of primary or secondary origin are associated with a wide spectrum of disease conditions[4,5]. Mitochondrial dysfunction not only involves alterations in structure or mitochondrial density but also in the quality and regulation of the respiratory system[6]. This qualitative element encompasses substrate control, coupling characteristics, post-translational modifications, cristae dynamics, and respiratory supercomplexes[7,8]. Therefore, accurate analysis of mitochondrial bioenergetics for experimental and diagnostic approaches to assess the energy metabolism of the cell is vital in health and disease.

Mitochondrial oxidative phosphorylation (OXPHOS) is a sequence of reactions within the respiratory system or electron transfer system (ETS) for the generation of cellular energy through adenosine triphosphate (ATP)[9]. The multi-enzymatic step to harness energy from electron flow through complexes I and II to complex IV generates an electrochemical proton gradient across the inner mitochondrial membrane, subsequently utilized for phosphorylation of adenosine diphosphate (ADP) to ATP via complex V (F_o-F_1-ATP synthase) (**Figure 1A**).

First, two-electron carriers are generated during the tricarboxylic cycle (TCA), glycolysis, and pyruvate oxidation: nicotinamide adenine dinucleotide (NADH) and dihydroflavine adenine dinucleotide ($FADH_2$). NADH is oxidized at complex I (NADH dehydrogenase), during which two electrons are transferred to coenzyme Q (quinone is reduced to quinol), while protons are pumped into the intermembrane space (IMS). Second, complex II (Succinate dehydrogenase) oxidizes $FADH_2$ and feeds the electrons to coenzyme Q without pumping protons. Third, at complex III (Cytochrome c oxidoreductase), electrons from coenzyme Q are transferred to cytochrome c while protons are pumped into the IMS. Fourth, cytochrome c transfers the electrons to complex IV (Cytochrome c oxidase), the final complex to pump protons, and where oxygen functions as an electron acceptor to assimilate protons, ultimately forming water. It is this oxygen that mitochondria consume and which can be measured by an oxygraph. Finally, the protons generated from complex I, complex III, and complex IV are used to rotate complex V, thereby generating ATP[9].

Importantly, electron transfer occurs not only in a linear fashion, otherwise denoted as the electron transport chain. Instead, electrons can be transferred to the Q-pool through multiple respiratory pathways and facilitate convergent electron flow. NADH-substrates and succinate, for example, can enter via complex I and complex II, respectively. Electrons from fatty acid oxidation can be donated via the electron transferring flavoprotein complex. Indeed, a comprehensive analysis of OXPHOS requires a holistic approach with appropriate fuel substrates (**Figure 1A**).

(Insert **Figure 1** here)

Analysis of mitochondrial OXPHOS capacity using HRR has become an instrumental biochemical method of diagnostic value not only for primary mitochondrial defects[10,11] but extending all other

realms of biology such as cancer and ageing[12]. HRR allows the determination of cellular respiration by the analysis of mitochondrial OXPHOS capacity, which directly reflects individual or combined mitochondrial respiratory complex deficiency, and indirectly is associated with cellular dysfunction and altered energy metabolism[9]. Methodologically, respiration measurements are performed using cells, tissue, or isolated mitochondria[11,13,14], with frozen material only partially suitable[15,16]. Frozen tissue is shown to have an intact ETS with maintained supercomplex stability[15]. Thus, as opposed to traditional TCA intermediates, respective substrates are directly fed into the ETS. However, coupling between the ETS and ATP synthesis is lost as the membrane integrity is compromised through freeze damage (ice crystal formation).

Respiration experiments normally take place at a physiological temperature of 37 °C for endotherms in either non-permeabilized or permeabilized cells or tissue. While the former considers the cytosolic metabolic context, the latter provides the energetic contribution of individual OXPHOS complexes and the ATPase through the addition of specific substrates (and inhibitors). The sequence and variation of substrates and inhibitors have led to the development of a diverse array of SUIT protocols[17] and assays[18] to address various scientific questions of OXPHOS function (reviewed under[12]). The basic protocol of cellular respiration assesses four different states: i) routine respiration—the respiration in a respective respiration media without any addition of substrates or inhibitors consuming but endogenous substrates. This state can reveal general OXPHOS or secondary-induced respiration defects caused, for example, by altered metabolite profiles. Next, the addition of the ATPase inhibitor oligomycin reveals the permeability of the inner mitochondrial membrane to protons, defined as ii) leak respiration. Subsequent titration of a protonophore such as the uncoupler carbonyl cyanide p-trifluoro-methoxyphenyl-hydrazone (FCCP) allows to determine the state at which ETS capacity is maximal in an open-transmembrane proton circuit mode, defined as iii) uncoupled respiration. Importantly, an uncoupled state can also occur by experimental interventions through excessive mechanical damage to the mitochondrial membranes. Conversely, the non-coupled state refers to respiratory uncoupling by an intrinsic mechanism that is physiologically controlled. Finally, complete inhibition of the ETS by addition of the complex III inhibitor antimycin and complex I inhibitor rotenone determines residual oxygen consumption (ROX) from non-mitochondrial oxygen-consuming processes (**Figure 1A–C**).

Mitochondrial bioenergetics consists of five distinct respiration states[19,20]. State 1 respiration is without any additional substrates or ADP, except for what is endogenously available. After the addition of ADP, but still, no substrates, state 2 respiration is achieved. When substrates are added, allowing electron transfer and ATP synthesis, state 3 respiration is reached. In this state, OXPHOS capacity can be defined at saturating concentrations of ADP, inorganic phosphate, oxygen, NADH- and succinate-linked substrates. State 4 respiration or LEAK respiration can be defined as a state without ADP or chemically inhibited ATP synthases while having sufficient substrates. Lastly, when all oxygen is depleted (anoxic) in a closed-chamber setting, state 5 respiration is observed.

Several methods exist to assess cellular energy states[14] with two devices dominating the current real-time assessment of OXPHOS through analysis of oxygen consumption, measured as the

function of the decrease in oxygen over time in a closed-chamber system with different applicability dependent on the experimental model and research question: the Oroboros 2k high-resolution respirometer and Seahorse XF extracellular flux analyzer. Both devices record the oxygen consumption rates as a decrease in picomoles (pmol) of oxygen (O_2) per second as an absolute value within the chamber or microplate well. The specific oxygen consumption per mass is obtained by normalizing the respective oxygen consumption in a specific buffer recipe per the number of cells (millions), tissue weight (mg), or protein amount.

The O2k (Oroboros Instruments) is a closed two-chamber system equipped with a polarographic oxygen sensor (abbreviated as chamber-based high-resolution respirometer: cHRR). Each experimental chamber holds 2 mL of liquid which is kept homogenous by magnetic stirrers. The polarographic oxygen sensor utilizes an amperometric approach to measure the oxygen: it contains a gold cathode, a silver/silver chloride anode, and in between a KCl solution creating an electrochemical cell upon which a voltage (0.8 V) is applied. Oxygen from the assay medium diffuses through a 25 µm fluorinated ethylene propylene membrane (O_2-permeable) and undergoes reduction at the cathode, producing hydrogen peroxide. At the anode, silver is oxidized by hydrogen peroxide, generating an electric current. This electric current (ampere) is linearly related to the partial oxygen pressure. The partial pressure of oxygen and the oxygen solubility factor of the assay medium are used to compute the oxygen concentration. Since oxygen partial pressure is dependent on experimental temperature and polarographic measurements are temperature-sensitive, fluctuations in temperature need precise (±0.002 °C) regulation by a Peltier heating block. Temperature can be controlled within a range of 4 °C and 47 °C.

The Seahorse XF extracellular flux analyzer (Agilent) is a plate-based system with 24- or 96-well microplate format in which three fluorescence electrodes measure oxygen consumption over time in each well (abbreviated as microplate-based high-resolution respirometer: mHRR). A maximum of four ports in the assay cartridge are available for automated injection during the assay. An assay contains multiple cycles, each with three phases: 1) mixing, 2) waiting, and 3) measurement. During the measurement phase, sensor probes are lowered into the microplate creating a temporarily closed chamber with 7–10 µL volume to measure emitted light. This light is emitted by polymer-embedded fluorophores on the tip of the sensor probes, which sense O_2 based on phosphorescence quenching. The intensity of the fluorescence signal is proportional to O_2 and influenced by the temperature of the sensor and assay medium. Therefore, accurate oxygen estimation requires a relative approach with a background well without any sample. Restoring oxygen concentration occurs during the mixing phase when the sensor moves up and down to mix the volume above the temporary chamber. Each cycle computes one oxygen consumption rate. Temperature can be controlled within a range of 16 °C and 42 °C.

In this study, basic protocols for HRR are provided to assess OXPHOS function in cells and tissues. HRR is the gold standard to assess cellular bioenergetics in primary and mitochondrially-associated diseases and general cellular metabolism.

(Insert **Figure 2** here)

PROTOCOL:

All animal experimentation is performed in accordance with the National Animal Experiment Review Board and Regional State Administrative Agency for Southern Finland. Male C57BL/6JOlaHsd mice (4–6 months-old) were used in this study. Consent for the use of human cell lines was obtained from the institutional ethics committee of the University of Helsinki.

1. High-resolution respirometry: Chamber-based respirometer (cHRR)

NOTE: The experiments in this section of the protocol were performed using O2k-Core: Oxygraph-2k (**Table of Materials**)

1.1. Calibration of oxygen sensors

1.1.1 Pre-run respirometers at 37 °C in 2.1 mL of mitochondrial respiration medium (MiR05, **Table 1**, solubility factor: 0.92) for >45 min and perform oxygen calibration as described[21]. Proceed if baseline variation is within ± 4 pmol/s.

NOTE: Large fluctuations in background signal could mean maintenance of the sensor membrane or traces of inhibitors remaining in the chamber from previous experimentation. An instrumental background oxygen flux correction is recommended prior to a batch of experiments[25].

1.1.2 Record oxygen calibration values to monitor the sensor membrane performance over time.

NOTE: This reveals sensor function and signal-to-noise stability and when sensor membrane maintenance is required. Dependent on ambient pressure, between 180–200 µmol of oxygen is solubilized in MiR05.

1.1.3 Remove all liquid in the chamber before the addition of any sample in the respiration medium.

NOTE: Evaluate the volume of respiration chambers to be exactly 2 mL regularly.

1.2. Preparation of cells for high-resolution respirometry

1.2.1. Culture HEK293 cells in 10 cm^2 diameter dishes in Dulbecco`s Modified Eagle`s medium (DMEM) with high glucose supplemented with 10% heat-inactivated fetal bovine serum (FBS), GlutaMax, Non-essential amino acids, and Na-Pyruvate[22] and uridine[23] to support OXPHOS-defective metabolism in an incubator at 37 °C at 5% CO_2.

NOTE: Any type of eukaryotic cell can be cultured. For most cell types, culturing a 10 cm^2 dish leads to sufficient cells (usually >3 x 10^6 cells). Routinely check for mycoplasma infection to avoid

effects on cellular metabolism and respiration.

1.2.2. Grow cells without exceeding 90% confluency (**Figure 2C**).

NOTE: Cells with >90% confluency may show growth-dependent inhibitory effects on respiration (if not synchronized or post-mitotic).

1.2.3. Wash the cells with 1x PBS, detach with 1 mL of warm 0.25% trypsin, deactivate trypsin by adding warm DMEM (5 mL/10 cm^2 plate) and count the cells with a hemocytometer.

1.2.4. Gently centrifuge the cell solution equaling 2.5 x 10^6 cells at 300 x *g* for 5 min, remove the supernatant completely, and resuspend in 2.5 mL of warm MiR05 (1 x 10^6 cells/mL)(**Figure 2A**).

1.2.5. For suspension cells, count and remove solution equaling 2.5 x 10^6 cells, pellet and continue as mentioned in step 1.2.4.

1.2.6. Run SUIT protocol for permeabilization optimization (step 1.6), permeabilized cell or tissue (step 1.5), or intact cells (step 1.7)

NOTE: For consistent results, it is recommended to keep cell concentration constant (e.g., 1 x 10^6 cells/mL). Although respiration is independent of cell density in the respirometer[24], substrates and inhibitors are in comparable concentration throughout experiments if cell numbers are kept constant.

1.3. Preparation of non-fibrous tissue (e.g., brain, liver) for high-resolution respirometry

1.3.1. Excise a homogenous piece of tissue, 30–40 mg in weight, or use the entire organ (mouse cerebellum in this case).

NOTE: If tissue is not immediately used, keep in 2 mL of ice-cold MiR05 allowing preservation for up to 2 h for most tissues. Individual tissue storage times need to be assessed in time series.

1.3.2. Blot the tissue dry with a Whatman filter paper (careful: soft tissue matter tends to stick).

1.3.3. Place the 30–40 mg tissue piece into an ice-cooled 2 mL polytetrafluoroethylene potter Elvehjem homogenizer.

1.3.4. Add an appropriate amount of MiR05 to obtain 20 mg/mL to maintain the tissue-to-buffer ratio. Keep the total amount >1.5 mL and <2 mL to avoid insufficient or excessive fluid for appropriate mechanical permeabilization.

1.3.5. Insert the pestle, lyse the tissue slowly by retracting the pestle carefully while avoiding the generation of a vacuum causing excessive tissue damage.

1.3.6. Perform 7 strokes in total (1x defined as one up- and downwards stroke) until lysed (apparent as a turbid liquid without major debris) (**Figure 2B**).

NOTE: The number of strokes for appropriate lysis needs to be tested for each tissue by assessing outer mitochondrial membrane integrity via cytochrome C response (step 1.5.11). Hard-to-lyse connective tissue or vessel parts might remain.

1.3.7. Decant the lysed tissue into a 15 mL centrifuge tube.

1.3.8. Wash the inside of the potter with an equal amount of MiR05 used in lysing step (e.g., 1.5 mL) and add to the 15 mL tube now containing 3–4 mL of MiR05 at 10 mg/mL tissue lysate.

1.3.9. Add 2 mL of plain MiR05 per chamber to warm to 37 °C.

1.3.10. Swirl the tube for equal distribution before pipetting 500 µL (equaling 5 mg) of each lysate per chamber slowly to minimize the stress from cold to 37 °C.

1.3.11. Wait >3 min for chamber contents to warm to 37 °C before closing the chamber. Remove excess fluid on top of the stopper (amount per chamber after closing: 4 mg).

1.3.12. Run the SUIT protocol for standard permeabilized (step 1.5).

1.4. Preparation of fibrous tissue (skeletal muscle, heart muscle) for high-resolution respirometry

1.4.1. Extract the hard tissue, remove the connective tissue and fat from the muscles using sharp forceps in 2 mL of ice-cold BIOPS (**Table 2**) under a dissection microscope.

1.4.2. Separate the fiber bundles (~4 mg) along the longitudinal axis with sharp forceps. Tease out the fibers sufficiently to obtain a mesh-like structure (**Figure 2B**).

NOTE: Proper mechanical fiber separation and permeabilization is indicated by the loss of the red pigment myoglobin and increased translucency.

1.4.3. Wash and permeabilize the fiber bundle in saponin (50 µg/mL in BIOPS, prepared fresh) for 20 min at 4 °C (fibers become translucent, indicating complete permeabilization, **Figure 2B**).

1.4.4. Wash the fibers twice in MiR05 for 5 min per wash at 4 °C.

1.4.5. Blot dry with filter paper and weigh before adding to the chamber filled with 2.1 mL MiR05.

1.4.6. Introduce stoppers without fully closing, then oxygenate the chambers with 2 mL of pure O_2 by using a 20 mL syringe and close the chambers by twisting the stoppers in a rotating motion.

Keep O_2 concentration between 300–500 µM during the experiment to avoid oxygen diffusion limitation.

1.5. Protocol for assessing routine respiration in cells or tissues

1.5.1. Add sample to the chamber as mentioned in steps 1.5.2–1.5.3.

1.5.2. Add 2.3 mL of warm MiR05 cell suspension (standard input: 1 x 10^6 cells/mL as in step 1.2 or 2 mg of tissue/mL as in step 1.3)

1.5.3. Skeletal and heart muscle (step 1.4): Add ~4 mg of saponin-permeabilized fibers to prewarmed 2.3 mL of warm MiR05 considering steps 1.4.4–1.4.6

1.5.4. Run chambers at 37 °C and a stirring speed of 700 rpm. Wait for >3 min to allow media to degas and close the chambers by twisting the stopper in a rotating motion. Peltier block stabilization indicates reaching the set temperature.

1.5.5. (OPTIONAL) Change the stirrer speed to 300 rpm to allow the remaining bubbles to escape through the capillary of the stopper.

1.5.6. Aspirate any excess liquid on top of the stopper. Wait for 10 min until a stable oxygen flux signal is achieved with any sample type to record routine/state 1 respiration, **Figure 1B**).

1.5.7. For respiration measurements in permeabilized cells and tissue, continue with step 1.6. For intact cells with step 1.8.

1.6. Protocol for OXPHOS analysis in permeabilized cells or tissues

1.6.1. Use lysed (permeabilized) tissue sample or permeabilize cells by adding 1 µL of digitonin (8.1 mM digitonin stock in dimethyl sulfoxide (DMSO)) for a final concentration of 5 µg/mL to permeabilize cells. The flux will drop and should stabilize at >5 min.

CAUTION: Digitonin is acutely toxic to the respiratory tract, in contact with skin, or when swallowed.

NOTE: Injection of all chemicals is performed with precision glass syringes. Use syringes only for indicated chemicals to avoid cross-contamination and thoroughly wash in water and EtOH after use. Blocked syringes may require ultrasonication in warm ddH_2O or a cleaning wire to dislodge any chemical clogs. Always retract a surplus of the respective stock solution into the syringe to avoid introducing air into the chambers. Inspect the inside of the chambers for the introduction of air after each injection. Record each step until flux plateaus.

1.6.2. Add in rapid succession: 5 µL of 0.4 M malate (M) for a final concentration of 1 mM, 5 µL of 2.0 M pyruvate (P; prepared freshly), for a final concentration of 5 mM, 4 µL of 2.5 M glutamate

(G) for a final concentration of 5 mM.

1.6.3. After previous flux plateaued, add 5 µL (10 µL for muscle tissue) of 0.5 M adenosine diphosphate (ADP, aliquots stored at -80 °C) for a final concentration of 1.25 mM.

NOTE: Tissue such as muscle might need a different concentration to reach saturation.

1.6.4. Add 5 µL of 4 mM cytochrome C (cytC) for a final concentration of 10 µM.

NOTE: Optional for cells to assess the quality of permeabilization.

1.6.5. Add 16 µL of 1.25 M succinate (S) for a final concentration of 10 mM. (OPTIONAL) Add 3 µL of 0.5 M ADP for a final concentration of 2 mM to control the saturation of ADP concentration.

1.6.6. For cells and non-fibrous tissue, add 2 µL of 1 mg/mL oligomycin (OM) for a final concentration of 1 µg/mL.

CAUTION: All ETS inhibitors used are highly toxic.

NOTE: Oligomycin may require titration for optimal concentration as it can repress ETS capacity and is omitted for muscle tissue. Reoxygenate here when muscle tissue is assayed and if O_2 is below 300 µM.

1.6.7. Titrate FCCP from a 2 mM stock, add 0.6 µL with subsequent 0.2 µL steps until no increase in respiration and respiration is maximally uncoupled (theoretical: non-coupled).

1.6.8. Add 1 µL of 1 mM rotenone (ROT) for a final concentration of 0.5 µM. Add 2 µL of 1 mg/mL antimycin (AM) stock for a final concentration of 1 µg/mL.

1.6.9. Reoxygenate the chambers to achieve a similar oxygen level (~150 µM) in all chambers by slowly lifting the plunger in twisting motion.

1.6.10. Add 5 µL of 0.8 M ascorbate for a final concentration of 2 mM immediately followed by 5 µL of 0.2 M N,N,N',N'-tetramethyl-p-phenylenediamine (TMPD) for a final concentration of 0.5 mM to assess complex IV activity (optional).

1.6.11. Add 5 µL of 4 M azide for a final concentration of 10 mM immediately when peak O_2 flux is reached with TMPD. Continue the run for >5 min to assay auto-oxidation of TMPD for complex IV base level calculation.

1.6.12. Recount the cells to confirm the cell count pre-run and continue with step 1.9.

NOTE: Digitonin-permeabilization (for cells only) needs to be titrated in trial experiments to reach maximal flux and not affect mitochondrial membrane integrity (see step 1.7). Permeabilized

samples (especially muscle tissue) with >10% increase in respiration rate after addition of cytochrome c should be excluded from further analysis due to outer mitochondrial membrane damage. A short-time dip in flux after the addition of EtOH-dissolved chemicals is expected.

1.7. Protocol to determine optimal permeabilization conditions for cells

1.7.1. Add cells as described in steps 1.2 and 1.5.2.

1.7.2. Take 10 µL of 10 mg/mL digitonin stock and add 10 µL of DMSO to dilute to 5 mg/mL.

1.7.3. Add 1 µL of rotenone (1 mM stock). Add 10 µL of succinate (2 mM stock) and 5 µL of ADP (0.5 M stock).

1.7.4. Titrate 1 µL of digitonin (2.5 mg per step) repeatedly until respiration does not increase further and is maximal.

NOTE: A decrease in respiration indicates a too high concentration of digitonin.

1.8. Protocol for OXPHOS analysis in intact cells

1.8.1. After routine respiration (step 1.6.1–1.6.6), add 2 µL of 0.01 mM oligomycin for a final concentration of 10 nM.

1.8.2. Titrate FCCP from 2 mM stock, add 0.6 µL with subsequent 0.2 µL steps until no further increase in respiration and respiration is maximally uncoupled (theoretical: non-coupled)

1.8.3. Add 1 µL of 1 mM rotenone for a final concentration of 0.5 µM. Add 2 µL of 1 mg/mL antimycin stock for a final concentration of 1 µg/mL.

1.8.4. Reoxygenate the chamber to the same oxygen level (~150 µM) by slowly lifting the plunger in twisting motion.

1.8.5. Add 5 µL of 0.8 M ascorbate for final concentration of 2 mM. Immediately add 5 µL of 0.2 M TMPD for a final concentration of 0.5 mM to assess complex IV activity.

NOTE: Prepare a fresh batch before any bigger set of experiments as TMPD is prone to auto-oxidation. The activity might decline over time when stored at -20 °C.

1.8.6. Add 5 µL of 4 M azide for a final concentration of 10 mM immediately when peak O_2 flux is reached with TMPD. Continue run for >5 min to assay auto-oxidation of TMPD for complex IV base level calculation.

1.8.7. Recount cells to confirm the cell count pre-run and continue with step 1.9.

1.9. Post-run sample collection

1.9.1. Collect exactly 1 mL of MiR05-suspension from each chamber with stirrers onto a 1.5 mL tube.

1.9.2. Centrifuge at 1000 x *g* for permeabilized cells or at 20,000 x *g* for tissue lysate. Remove the supernatant and freeze the pellet at -80 °C for further processing (section 3).

1.10. Analysis of SUIT protocols

1.10.1. Analyze oxygen flux (pmol/s, normalized to input) at each plateau after adding a substrate or inhibitor (**Figure 1C** and **Figure 3A**). Export the values to a spreadsheet.

1.10.2. Subtract the residual oxygen consumption (ROX, **Figure 1C** and **Figure 3C**) value from all values of each experimental run. Subtract azide residual respiration from TMPD to obtain complex IV respiration.

1.10.3. Plot the absolute values normalized for cell (**Figure 3A**,**B**) or tissue input (**Figure 5A,B**). Calculate the flux control ratios (step 1.11) or normalize them to protein input (**Figure 3C**).

1.11. Flux control ratio calculation

1.11.1. Acquire an index of respiratory function and coupling control using flux control ratios (FCR)[9,26].

NOTE: This allows assessing intrinsic mitochondrial quality, independent of mitochondrial quantity. In addition, flux control ratios (FCR) are comparable within the same cell lines allowing for reagent quality control (respective FCRs are obtained through the indicated numbered reference values in **Figure 1B–D** and **Figure 3C**).

1.11.2. Calculate the respiratory control ratio for the coupling of OXPHOS to LEAK using Equation 1.

Equation 1: $FCR_{ADP} = 5/6 = State\ 3 / State\ 4$

1.11.3. Calculate the FCR to assess NADH-dependent respiration using Equation 2

Equation 2: $FCR_{state\ 3\ (I)} = 3/5 = State\ 3\ (I) / State\ 3\ (I+II)$

1.11.4. Calculate the FCR to assess Succinate-dependent respiration using Equation 3.

Equation 3: $FCR_{state\ 3\ (II)} = 8/7 = S_{rot} / ETS_{capacity}$

1.11.5. Calculate the FCR to assess coupled to uncoupled using Equation 4.

Equation 4: $FCR_{coupled/uncoupled} = 5/7 = State\ 3\ (I+II) / ETS_{capacity}$

1.11.6. To test mitochondrial outer membrane integrity, use Equation 5.

Equation 5: % mitochondrial outer membrane damage = 3/4 = State 3 $_{(I)}$ / State 3 $_{(I)\ with\ cyt\ c}$

2. High-resolution respirometry: Microplate-based respirometer (mHRR)

NOTE: The experiments in this section of the protocol were performed using Seahorse XFe96 Extracellular Flux Analyzer (**Table of Materials**)

2.1. Cell culture

2.1.1. Culture any type of cell. Adherents (e.g., collagen, laminin) might be used to facilitate cell attachment. Here, HEK293 cells are cultured as before (step 1.3).

2.1.2. The day before the experiment, detach the cells and transfer them into a designated mHRR 96-well microplate to obtain ideal confluency on the day of the experiment (80%–100%) (**Figure 2C**).

NOTE: For mHRR, microplate cell densities are critical. Individual growth properties of cells lines or treatments affecting growth need to be corrected to amount to comparable confluency on the day of the experiment.

2.2. Preparation of cells for high-resolution respirometry

2.2.1. Harvest and resuspend the cells sufficiently prior to seeding

NOTE: It is recommended to seed cells from the same dilution for replicates.

2.2.2. Seed the cells according to growth rates of individual cell lines or growth properties under treatment.

NOTE: Optimize on a 96-well microplate and extrapolate the cell density to assay 96-well (surface area of 0.106 cm^2). In this setup, 7 x 10^4 HEK293 WT cells were seeded per well of a 96-well. The first and last columns of the 96-well plate are used for protein determination (**Figure 2C**). The four corner wells should not contain any cells and are used for experimental background correction. Ideally, wells close to the edges are empty to minimize edge effect (e.g., cells show altered growth from temperature effects) **(Figure 2C**,**D**).

2.3. Preparation of sensor plates, loading of inhibitors

2.3.1. On the day of the assay, supplement 38.8 mL of medium with 0.4 mL of 1 M Glucose, 0.4 mL of 200 mM Glutamine, and 0.4 mL of 100 mM Na-Pyruvate.

NOTE: mHRR respiration requires a specialized non-buffered DMEM medium at pH 7.4. In general, 40 mL should suffice for one experiment with one 96-well microplate.

2.3.2. Warm the respiration assay medium to 37 °C and exchange the cell culture medium for the respiration assay medium by washing twice with 80 µL per well.

2.3.3. Set the plate with the cells in a 37 °C incubator without CO_2 for 60 min prior to the assay.

NOTE: This step is essential to degas the plate as CO_2 can affect respiration results, and serum in the medium can produce bubbles during the assay.

2.3.4. Prewarm inhibitor aliquots for OM, FCCP, ROT, and AM to 37 °C and take the sensor plate out of the incubator.

2.3.5. Dilute OM, FCCP, ROT, and AM in 3 mL of assay medium to a final well concentration of 1.5 µM, 1.125 µM, and 1 µM, respectively. Fill into separate ports as indicated in **Figure 2E**.

NOTE: A multichannel pipette is recommended to fill the sensor cartridge. Since pressurized air is used to inject compounds, all ports must be filled with an equal amount of liquid volume whenever a port is filled with a compound. ROT and AM can be combined in one port. Inhibitors can be dissolved in EtOH or DMSO.

2.3.6. Inspect the injection ports and verify an even loading volume for each port.

NOTE: All ports contain a hole at the bottom for injection. Care should be taken when moving the sensor plate. Air bubbles can be removed using a needle.

2.4. Protocol for oxygen assessment in intact cells

2.4.1. On the day before the assay, perform steps 2.4.2–2.4.7.

2.4.2. Aliquot 20 mL of the calibrant solution into a 50 mL conical tube.

2.4.3. Open the Extracellular Flux Assay Kit and remove the contents.

2.4.4. Place the sensor cartridge inverted next to the utility plate. Pipette 200 µL of calibrant solution into each well of the utility plate.

2.4.5. Attach the sensor cartridge onto the utility plate paying attention that all sensors are submerged.

2.4.6. Set the plate into a 37 °C incubator without CO_2 overnight or a minimum of 12 h. Verify

that the humidity inside the incubator is sufficient to prevent evaporation of the calibrant.

2.4.7. Turn on the microplate-based system and computer to be ready to use the next day (the machine requires a minimum of 3 h to equilibrate to 37 °C prior to conducting an assay).

NOTE: For signal stability, increase measurement points to 6 instead of 3 measurement cycles per respiratory state. Each cycle consists of 3 min of mixing and 3 min of measuring.

2.4.8. On the day of the XF assay, perform steps 2.4.9–2.4.20.

2.4.9. Verify the confluency of the cell culture plate, the morphology of the cells, and that background wells are empty.

2.4.10. Wash the cells with the prepared respiration medium as mentioned in steps 2.4.11–2.4.12.

2.4.11. Remove all but 20 µL of the culture medium from each well. Remove 55 µL if the culture medium was 80 µL due to evaporation overnight (approximately 5 µL).

2.4.12. Wash twice with 90 µL of assay medium. Finally, add 100 µL of assay medium. The end volume should be 120 µL.

NOTE: A multichannel pipette is recommended for this step to ensure the same washing procedure has been applied to each experimental condition (depends on the plate setup). When aspirating, tilt the plate to a 45° angle and always slide the pipette tips along the corner of the well for aspiration and injection of liquids. It is imperative to take care during the washing as certain cells may easily detach from the bottom of the cell culture plate.

2.4.13. Set the plate in a 37 °C incubator without CO_2 for 60 min prior to the assay.

2.4.14. Retrieve the hydrated sensor cartridge plate from the CO_2-free incubator.

2.4.15. Discard the old calibrant solution and replace it with fresh calibrant solution, prewarmed to 37 °C.

2.4.16. Prepare inhibitors and assay medium (3 mL per inhibitor for a total of 12 mL of assay medium) and use a pipette reservoir for the inhibitor loading into ports.

2.4.17. Open the software and run a pre-designed or new template. Fill the plate map, adjust the titrations and measurement cycles, and then press **Start** to initiate the calibration of the optical sensors.

2.4.18. Remove the lid from the loaded cartridge and place it in the slot that automatically slides out of the machine, verifying that the markings on the lower right corner of the plate line up with

the triangle on the lower right corner of the slot.

2.4.19. Click on **Continue** to perform automatic calibration, lasting approximately 20 min.

2.4.20. After calibration, remove the utility plate containing the calibrant.

2.4.21. Remove the lid from the microplate containing the cells and place the plate in the slot when prompted by the machine. Click on **Continue** to start the run.

2.5. Post-run sample collection

2.5.1. Take the plate out of the machine, carefully remove the remaining assay media without disturbing the cells and freeze the entire plate at -80 °C for further processing (section 3).

3. Determination of protein using the bicinchoninic acid assay (BCA assay)

3.1. Prepare diluted bovine serum albumin (BSA) in buffer used for protein extraction and compatible with BCA: 2 mg/mL, 1.5 mg/mL, 1 mg/mL, 0.5 mg/mL, 0.25 mg/mL and 0 mg/mL for standard curve in duplicates.

3.2. Extract proteins by resuspending in an appropriate lysis buffer (e.g., RIPA) with 20 µL per well for mHRR or 100 µL per pellet contained within a 1.5 mL tube for cHRR.

3.3. Incubate the mHRR plate or 1.5 mL tube containing protein lysates for 30 min on ice.

3.4. Centrifuge the 1.5 mL tube containing the protein lysate at 4 °C at 20,000 x *g* for 20 min and transfer the resulting supernatant to a new clean 1.5 mL tube.

3.5. Use 10 µL per sample in duplicates and standards in a microtiter plate. Add 200 µL of BCA working reagent and incubate for >15 min.

3.6. Read in a standard spectrophotometer at a wavelength of 562 nm and calculate the protein concentrations using a BSA standard curve.

3.7. Normalize the respiration results to the protein concentration.

NOTE: Normalization to protein amount allows to corroborate cell seeding densities or wet weight input. The extracted proteins are suitable for subsequent immunoblotting against subunits of the ETS for example but do not fully represent the native sample (e.g., loss of phosphorylation sites).

REPRESENTATIVE RESULTS:

Here, we provide protocols to determine the mitochondrial bioenergetics in eukaryotic cells, non-fibrous tissue (e.g., cerebellum), and fibrous tissue (e.g., skeletal muscle). For eukaryotic

cells, HEK293 with CRISPR-engineered knockout of two different proteins associated with mitochondrial translation resulting in multiple ($CRISPR^{KO1}$) and severe/complete OXPHOS deficiency ($CRISPR^{KO2}$) were measured with either cHRR (**Figure 3A–C**) or mHRR (**Figure 3A–D**). For cHRR, HEK293 cells were digitonin-permeabilized, and respiration experiments performed following the standard protocol (step 1.5–1.6) and were successfully recorded (**Figure 3A**). $CRISPR^{KO1}$ shows impaired and $CRISPR^{KO2}$ no respiration compared to WT when normalized to cell input amount (**Figure 3B**). Protein amount was determined from collected samples (section 3), and values of routine respiration normalized to protein amount to calculate absolute values and respective FCRs (**Figure 3C**, the meaning of each FCR is detailed in discussion). Optimal sample amounts produce fluxes of 80-160 pmol/s per mL. Ideally, the amount of cells or tissue is sufficient to generate a significant flux (20 pmol/s for cHRR) to reduce background noise while evading excessive reoxygenation during an experiment. In low respiring (e.g., white adipose fat, white blood cells) or hard-to-obtain samples (e.g., iPS-differentiated neuronal lineages), fluxes of 20 pmol/s per mL are sufficient in ideal working conditions.

(Insert **Figure 3** here)

Next, we used mHRR with the same cells in a standard protocol (2.1–2.5), confirming the OXPHOS deficiencies (**Figure 4A**). In addition, ECAR values were increased for severe/complete OXPHOS deficiency ($CRISPR^{KO2}$), suggesting compensation of mitochondrial oxidative phosphorylation deficiency in HEK293 cells with specific mitochondrial translation deficiency through increased glycolysis resulting in lactate production (**Figure 4A**). Protein amount was determined from the microwell plate (section 3), and values obtained were normalized to protein amount (**Figure 4B**) and quantified (**Figure 4C**). Microplate-based systems are notorious for high intra-well variation. High variability between replicates can occur when the optimal seeding density has not been achieved; cells get detached during the washing steps of replacing the cell culture medium with assay medium, or improper pipetting technique such as the introduction of air bubbles or aspiration of varying volumes. Extended measurement times (6 measurement cycles) are recommended with mHRR to allow for stabilization of flux in media (**Figure 1B** and **Figure 4A**). Low fluxes cause high variation, and dependent on cell type, flux might be too close to background noise (up to 10–15 pmol/s). Low-respiring (e.g., fibroblasts) or exceptionally large cells might produce insufficient oxygen flux above background noise level in the 96-well microplate format even at 90% confluency. The 24-well microplate mHRR format or cHRR should be considered. Minimal changes in oxygen flux can also indicate faulty handling of loading the inhibitors, such as empty, incorrectly, or variably filled ports. The use of specific pipette tips that enter ports sufficiently during loading the chemicals is recommended to allow chemicals to reach the individual port (**Figure 2E**).

(Insert **Figure 4** here)

An example experiment for non-fibrous tissue preparation (step 1.3 and 1.5–1.6) using mouse cerebellum (**Figure 5A**) and fibrous tissue preparation (step 1.4 and 1.5–1.6) using mouse skeletal muscle (soleus) is shown (**Figure 5B**). In general, uncoupled respiration does not exceed OXPHOS capacity in mouse samples. For mouse cerebellum, OXPHOS capacity decreased when comparing

with maximal ETS capacity. LEAK respiration increased under physiologically controlled circumstances versus chemically induced (oligomycin). This could be due to the fact that endogenous available ADP is still phosphorylated to ATP, whereas with chemical induction, proton leak is maximal, resulting in an overestimation of LEAK respiration. In contrast to the cerebellum, the soleus was tested at hyperoxic conditions to avoid oxygen diffusion limitation and shows three times higher OXPHOS capacity. NADH-dependent respiration is different when analyzing specific types of tissue, with the soleus having more capacity to respire through the addition of succinate than the cerebellum. Both types of tissue show minimal ROX.

(Insert **Figure 5** here)

FIGURE AND TABLE LEGENDS:

Figure 1: Mitochondrial oxidative phosphorylation and specific substrate and inhibitor protocol. (**A**) Mitochondrion and scheme of the electron transfer system (CI-CIV) and mitochondrial F_0F_1 ATPase (CV). (All structures from PDB. The figures only depict all substrates and inhibitors described here). (**B**) Sample trace of oxygen flux in intact HEK293 cells using standard protocol in a mHRR device. (**C**) Sample trace of oxygen flux in intact HEK293 cells using standard protocol in a cHRR device. (**D**) Sample trace of oxygen flux in permeabilized human fibroblasts from a healthy donor with respective SUIT protocol. Abbreviations: 1 = Routine respiration of intact cells; 2 = State 2; 3 = State 3(I); 4 = State 3(I) with cytC; 5 = State 3 (I+II); 6 = Leak(OM); 7 = ETS capacity; 8 = S(ROT); 9 = ROX; 10 = TMPD; 11 = Az. ROT = Rotenone, AM = Antimycin, ATP = Adenosine triphosphate, Az = Azide, OM = Oligomycin, FCCP = Carbonyl cyanide p-trifluoro-methoxyphenyl-hydrazone; Asc = Ascorbate, TMPD = N,N,N',N'-tetramethyl-p-phenylenediamine, Succ = Succinate, M = Malate, P = Pyruvate, ADP = Adenosine diphosphate, NAD = Nicotinamide adenine dinucleotide, IMS = Intermembrane space, FAD = Flavin adenine dinucleotide.

Figure 2: Workflow for cell and tissue preparations for cHRR, and cell preparation for mHRR respirometry. (**A**) Outline of provided protocols. (**B**) Mammalian cells (step 1.2): HEK293 pellet equaling 3 x 10^6 cells (left panel). Non-fibrous tissue (step 1.3): Preparation of murine cerebellum lysate in 2 mL Teflon potter (middle panel). Saponin-induced skeletal muscle permeabilization (step 1.4) right panel) for cHRR respirometry. (**C**) Standard microplate seeding layout (step 2.4) and confluency check for the analysis of eukaryotic cells (HEK293) for mHRR respirometry. (**D, E**) Scheme of injection port loading for mHRR respirometry (step 2.4).

Figure 3: Representative standard protocol oxygen consumption traces from cHRR using HEK293 cells with combined OXPHOS deficiency. (**A**) Raw oxygen consumption traces of WT HEK293 cells and HEK293 cells with CRISPR-mediated mitochondrial translation defects causing multiple OXPHOS deficiency ($CRISPR^{KO1,2}$). (**B**) Overlaid cell-input-normalized oxygen consumption traces from (**A**). (**C**) Protein-normalized quantification of 2 independent experiments (mean and SD) and respective FCRs. Comparisons between conditions were done by ANOVA and a posteriori Tukey's test or a Student's *t*-test. Significances: **** $p < 0.0001$; *** $p < 0.001$; ** $p < 0.01$; * $p < 0.05$.

Figure 4: Representative standard protocol oxygen consumption traces from mHRR using HEK293 cells with combined OXPHOS deficiency. (**A**) Raw oxygen consumption traces of WT HEK293 cells and HEK293 cells with CRISPR-mediated mitochondrial translation defects causing multiple OXPHOS deficiency ($CRISPR^{KO1,2}$). (**B**) Respective extracellular acidification rates (ECAR) from (**A**). (**C**) Protein-normalized oxygen consumption traces of WT HEK293 cells and HEK293 cells with CRISPR-mediated mitochondrial translation deficiency causing multiple OXPHOS deficiency ($CRISPR^{KO1,2}$). (**D**) Protein-normalized quantification of wells (n = 8 per genotype; mean and SD). Comparisons between conditions were done by ANOVA and a posteriori Tukey's test. Significances: **** $p < 0.0001$; *** $p < 0.001$; ** $p < 0.01$; * $p < 0.05$. Abbreviations: see **Figure 1**.

Figure 5: Representative traces of oxygen consumption for non-fibrous (A) and fibrous (B) tissues for cHRR. (**A**) Wet weight tissue-normalized oxygen consumption trace of mouse cerebellum prepared as described (step 1.3). (**B**) Wet weight-tissue-normalized oxygen consumption trace of mouse soleus muscle as described (step 1.4). Blue line shows respective oxygen concentration and injection points. Abbreviations: see **Figure 1**.

Table 1: Mitochondrial respiration medium MiR05 composition adjusted to pH 7.1[27]**.**

Table 2: Relaxing and biopsy preservation solution (BIOPS) composition adjusted to pH 7.1[28].

DISCUSSION:

Mitochondrial bioenergetics has been studied with Clark-type oxygen electrodes. A lack of resolution and throughput, however, warranted for technological advancement. To date, the O2k (referred to as cHRR) and Seahorse XF96 Flux Analyzer (referred to as mHRR) have been widely adopted in the field of cellular bioenergetics. Here, we present a comprehensible collection of protocols for the analysis of cellular energy metabolism via assessment of mitochondrial respiration using either cHRR or mHRR, discuss key benefits of each device and provide practical guidance. The protocols provided here encompass mammalian cells, fibrous (hard) tissues such as skeletal and heart muscle, and non-fibrous (soft) tissues such as brain and liver and are applicable to similar types of sample material.

While both HRR methods result in comparable data for mammalian cells as exemplified with HEK293 with multiple OXPHOS deficiency, general working principles and technical setup of the devices render them suitable for different applications. The mHRR setup allows automated data acquisition and has the high-throughput capability with a 24- or 96 multi-well setup requiring minimal sample amounts. However, the low experimental volume and well surface, in addition to the use of oxygen-permeable polymers (polystyrene), can cause high intra-well variation (especially in the 96-well plate setup), promoting the use of ≥6 wells per condition for reproducible results. In contrast to the cHRR based-polarographic oxygen sensor, no oxygen is consumed by the sensor probes of the mHRR, which utilizes quenched phosphorescence O_2 sensing. As the mHRR is a semi-closed system, ambient O_2 can diffuse into the respiration medium, exposing the sample and the probe to oxygen. When the piston-like sensor probe lowers, a temporarily sealed and isolated chamber is created to amplify changes in O_2

concentration and measure oxygen consumption. Subsequently, a mathematic model is employed to accurately compute oxygen consumption rates by estimating the back diffusion of O_2. However, the drawback is that the algorithm also amplifies noise[29]. The microplate setup utilizes non-reusable specialized ports and plates requiring optimal cell seeding density. The mHRR oxygen sensor probes measure lateral O_2 diffusion in three distinct areas per well equivalent to the size of the probe (~1 mm); therefore, a uniformly distributed cell monolayer is crucial to determine accurate oxygen consumption rates. If any significant gaps are present when observing the cell distribution, incorrect oxygen consumption rates will be computed, resulting in a high variance of well replicates. Taking this into consideration, mHRR is semi-automated and ideally adaptable for high-throughput cell or small-organism-based studies (e.g., *C. elegans*) with recurring screenings. The cHRR respirometers setup is based on a two-chamber system with polarimetric measurement of oxygen. In the closed-based system, ambient O_2 cannot diffuse into the respiration medium; thus, a decline in O_2 concentration reflects oxygen consumption of the biological sample. As the cHRR polarographic oxygen sensor consumes oxygen, diffusion of free O_2 is essential, making it difficult to minimize chamber volume (2 mL, new cHRR devices 0.5 mL) and requiring constant stirring to ensure homogeneity of the respiration medium. Consequently, larger sample volumes are required to generate sufficient oxygen flux. Due to direct access to the chambers and manual titration, any respiration protocol is adaptable and based on widely commercially available chemicals results in exceptionally low running costs. In addition, *ad hoc* operability allows adapting a SUIT protocol by titration during an experiment and is important in single-time patient-derived samples. Partial automation is feasible using a titration-injection micropump, which enables programmable SUIT protocols. Although restricted to two samples per cHRR device, experienced users will run several devices in parallel. The benefit of the versatility of assay development and software environment comes with the need for more specific training to operate these devices and user-dependent maintenance (e.g., calibration of polarographic oxygen sensors) in order to acquire reproducible data. For advanced applications, additional modules are attachable to the cHRR devices to record pH, fluorescent module to assay membrane potential via safranin[30], H_2O_2 via AMPLEX red[24], and calcium levels[31].

Both devices require specialized respiration media. mHRR uses a commercially available serum-free growth medium, avoiding the use of bicarbonate, which degasses under low CO_2 conditions and is essential if extracellular acidification rate (ECAR) is of importance. During glycolysis, pyruvate is converted into lactate, which dissociates into lactic acid and protons. This increased proton concentration causes the pH to decrease, which is recorded as ECAR. A more elaborate analysis of ECAR is possible with the glycolysis stress test. This assay consists first of adding saturating glucose levels to measure the basal glycolytic rate. After inhibition of the ATP synthase complex with oligomycin, the maximal glycolytic rate is revealed. The final step is to measure non-glycolytic acidification by injecting 2-deoxy-glucose, which inhibits glycolysis via competitive binding to hexokinase and phosphoglucose isomerase[32]. Other kit-based protocols available encompass glycolysis, fatty acid oxidation, and glutamine oxidation. Here, we used the standard protocol to measure basal respiration, ATP-linked respiration, proton leak, maximal respiration, spare respiratory capacity, and non-mitochondrial respiration (**Figure 4A–C**). An approach of utilizing both the standard respiration protocol in conjunction with the glycolysis stress test would give insight into aerobic and anaerobic energy pathways providing an overview of cellular

respiration.

Cellular bioenergetics is usually accessed in adherent cells with the microplate mHRR setup. Dependent on cell type, specialized coating for adherence (e.g., poly-D-lysine, gelatin, etc.) might be required (for suspension cells) as well as for loosely adherent cells as they may detach from the bottom of the well measurement cycles[33]. In contrast, cHRR measurements require constant stirring, allowing respiratory measurement for any biological sample. For each device, optimization such as titration of inhibitors (and substrates) for tissue and cell lines to assess inhibitor-susceptibility (dose-response curves) is required. Inhibitor concentrations should be trialed in any experimental model to use the lowest fully inhibiting concentrations and to prevent unspecific inhibition as well as unnecessary chamber contamination. Generally, 0.25 µM rotenone, 0.5 µg / mL Oligomycin A, 0.5 µg / mL antimycin are sufficient for most applications and sample amounts. For reproducibility, prepare single-use drugs in sufficient quantities for the entire planned experiments (e.g., mouse groups) and keep sample input constant within a specific tissue or cell line. In cHRR, traces of inhibitors remaining in the chambers will alter flux without any indication to the operator. Particularly rotenone traces are difficult to evade and require sufficient washing with a minimum chamber (and stopper) cleaning, which encompasses washing 4x with ddH_2O, 2x 70% EtOH (96% purity sufficient), 1x 100% EtOH, 1x 70% EtOH. Washing requires turning stirrers and keeping EtOH-steps for > 5 minutes each. To prevent bacterial contamination, 70% EtOH is kept in all chambers when machines are not in use. Potential residual contaminates can be quenched by the addition of unused tissue lysate. In a mHRR experiment, certain chemicals may interact with the essential single-use plasticware[34]. Respiratory data obtained via a permeabilized protocol give insight into the ETS, whereas an intact protocol provides insight into mitochondrial properties such as mitochondrial efficiency. Indeed, general mitochondrial energy properties can give the same outcome, but underlying electron transfer between complexes may be altered. This would reflect altered mitochondrial energy metabolism and requires a permeabilization protocol to access the respiratory complexes. Similarly, different tissues and cells show altered substrate dependency when assessing respiratory characteristics. For instance, glycolytic muscle fibers are known to rely primarily on glycerol-3-phosphate for energy delivery, whereas oxidative muscle fibers possess a two-fold higher electron transfer capacity from NADH oxidation[35,36]. On the same note, heart mitochondria, liver, brown adipose tissue can utilize fatty acids to synthesize ATP, and in turn, the brain can use ketone bodies, predominantly formed by fatty acid oxidation[36–38]. Therefore, determining mitochondrial characteristics requires a holistic approach as opposed to the standard glucose-dependent respiration. mHRR usually encompasses assessing intact adherent cells, although permeabilization is achievable (e.g., mutant recombinant perfringolysin O that selectively permeabilizes the cell membrane[39]). However, these methods come with increased complexity due to the limitation of four injection ports. In contrast, correctly lysed non-fibrous tissue lysates and any cell type are usually problem-free for cHRR. Normally, assaying tissue with the mHRR is not feasible; however, approaches using isolated mitochondria from a tissue have been established[40,41].

Important to note is that normalization to whole protein content neglects absolute mitochondrial amounts. Comparison of experimental groups under various treatments can differ significantly

(e.g., 30 days high-protein diet-fed rats showed a 2.5-fold increase in mitochondrial content in liver[42]), particularly in tissue susceptible to intracellular lipid accumulation such as brown adipose tissue, liver, and skeletal muscle. In these situations, it is also recommended to assess several mitochondrial markers as an approximation for mitochondrial mass, such as mtDNA copy number[43], citrate synthase activity[10], and ubiquitous mitochondrial proteins (e.g., VDAC1, TOM20). In combination, this allows to distillate whether an altered respiratory function is attributed to mitochondrial quantity, quality, integrity, or a combination thereof. Another method that is complementary to this is the implementation of FCRs. FCRs give insight into different respiratory states independent of mitochondrial content. FCR_{ADP} derives whether altered LEAK or OXPHOS change the efficiency of the mitochondria to phosphorylate ADP. $FCR_{state\ 3\ (I)}$ reflects to what degree the sample is dependent on complex I as a comparison to complex II. $FCR_{state\ 3\ (II)}$ compares succinate-dependent respiration with ETS and provides an index for mitochondrial respiration derived from complex II. $FCR_{coupled/uncoupled}$ is a ratio providing the coupling control between OXPHOS and ETS, with a ratio of 1 having no spare respiratory capacity left. The mitochondrial outer membrane integrity can be assessed through the addition of exogenous cytochrome c. Cytochrome c is localized in the intermembrane space, where it facilitates the transfer of electrons between complex III and complex IV. If the outer mitochondrial membrane is damaged, cytochrome c leaks out of the mitochondria, not contributing to respiration anymore. Restoring this imbalance can be achieved via the addition of exogenous cytochrome c, consequently increasing respiration (**Figure 1A, D; 5B**). Complex IV activity is measured individually with TMPD after complete inhibition of OXPHOS. Baseline O_2 flux will decline as the O_2 concentration falls because TMPD oxidation is O_2 concentration-dependent. Hence after ROX assessment, all chambers are oxygenated to equal oxygen level (150 µM). Linear regression of data points from signal after addition of azide can be used to interpolate chemical and O_2-dependent background of complex IV activity assay. ROX should be subtracted from all respiration values to correct for non-mitochondrial oxygen consumption.

Biologically, ROX in the case of isolated mitochondria can be lower than with permeabilized or intact cells/tissue. In general, residual respiration is caused by the activity of oxidase enzymes, with cells and tissue having more autoxidizable substances than isolated mitochondria[44]. Furthermore, with intracellular membrane structures still intact, the difficulty of oxygen to permeate through cell membranes increases due to its negative charge. Consequently, diffusion through cellular membranes and intracellular availability of oxygen can be affected, resulting in ROX. However, isolation of mitochondria has been shown to disrupt mitochondrial morphology, increase mitochondrial hydrogen peroxide production, along with altered mitochondrial respiratory function[45]. While isolation of functional mitochondria allows for specific normalization and might be required in certain conditions, the isolation process is time-consuming, usually requires more material, and might not preserve mitochondrial heterogeneity. For this reason, we have refrained from including mitochondrial isolation in this study. However, for skeletal or heart muscle, isolation of mitochondria or saponin-treatment of fibers is essential for respiration measurements. As autolytic processes occur very quickly after euthanasia, fast tissue extraction and adhering to comparable timing for preparations between individual experiments is recommended.

In our experiment in mammalian cells assessed with both devices, comparable results were obtained. However, basal respiration was higher for cHRR compared to mHRR, for example. Apart from numerous technical aspects such as chamber volume, stirring, and differing signal integration, biological reasons such as non-attached cells causing loss of cell contact, timing, altered respiration medium could inflict the unexplained observed differences. Consequently, respiration protocols in a general and individual substrate and inhibitor concentrations are not interchangeable between systems for the presented reasons, which could be technical in nature (e.g., titration) and generally differing assay reagents (e.g., respiration media, chemical absorbances of glass or polymers). To ensure highest reproducibility, several technical considerations and recommendations encompass (i) the use of single-use aliquots to minimize cross-contamination or freeze-thaw cycles, (ii) appropriate storage of all chemicals (e.g., ADP at -80 °C for prolonged stability, pyruvate prepared freshly and light-sensitive chemicals in the dark), (iii) regular and rigorous re-testing of chemicals for efficacy (e.g., evaporation-inflicted concentration changes, storage-induced TMPD activity loss) and (iv) extensive cleaning to remove and trace chemical. Considerations on the reproducibility of longitudinal studies (over several years) would require monitoring the device performance and ensuring the stability of reagents over time.

Finally, novel technology based on combined potentiometric (pH) and amperometric (O_2) measurements through ruthenium oxide-based electrodes could catalyze a paradigm shift in current tools, allowing studying cellular metabolism in culture and *in vivo*[46]. Although current methods allow predominantly *ex vivo* and *in vitro* assessment of cellular metabolism, delayed fluorescence enables *in vivo* analysis of mitochondrial oxygen as a measure of mitochondrial function[47]. Similarly, microfluidics-based respirometry shows promise in higher sensitivity, requiring only a few hundred cells[48]. While new methodologies are on the horizon, to date, high-resolution respirometry remains the gold standard to assess cellular respiration capacity for which quintessential protocols are provided here, applicable to most cells, tissues, and organisms to study mitochondrial respiration.

ACKNOWLEDGMENTS:
This work was supported by funding from the Academy of Finland (C.B.J), the Magnus Ehrnroot Foundation (C.B.J), and a Doctoral fellowship of the Integrated Life Sciences Graduate School (R.A.).

DISCLOSURES:
No conflict of interest to disclose.

REFERENCES:
1. McBride, H. M., Neuspiel, M., Wasiak, S. Mitochondria: More than just a powerhouse. *Current Biology*. **16** (14), 551–560 (2006).
2. Mehta, M. M., Weinberg, S. E., Chandel, N. S. Mitochondrial control of immunity: Beyond ATP. *Nature Reviews Immunology*. **17** (10), 608–620 (2017).
3. Spinelli, J. B., Haigis, M. C. The multifaceted contributions of mitochondria to cellular metabolism. *Nature Cell Biology*. **20** (7), 745–754 (2018).

4. Gnaiger, E. Capacity of oxidative phosphorylation in human skeletal muscle. New perspectives of mitochondrial physiology. *International Journal of Biochemistry and Cell Biology*. **41** (10), 1837–1845 (2009).
5. Gorman, G. S. et al. Mitochondrial diseases. *Nature Reviews Disease Primers*. **2**, 1–23 (2016).
6. Boushel, R., Gnaiger, E., Schjerling, P., Skovbro, M., Kraunsøe, R., Dela, F. Patients with type 2 diabetes have normal mitochondrial function in skeletal muscle. *Diabetologia*. **50** (4), 790–796 (2007).
7. Cogliati, S. et al. Mitochondrial cristae shape determines respiratory chain supercomplexes assembly and respiratory efficiency. *Cell*. **155** (1), 160–171 (2013).
8. Kühlbrandt, W. Structure and function of mitochondrial membrane protein complexes. *BMC Biology*. **13** (1), 1–11 (2015).
9. Gnaiger, E. *Mitochondrial pathways and Respiratory control*. *An introduction to OXPHOS analysis. Bioenergetics communications*. 5th ed, **2**, Steiger Druck GmbH, Axams, Austria (2020).
10. Jackson, C. B. et al. Mutations in SDHD lead to autosomal recessive encephalomyopathy and isolated mitochondrial complex II deficiency. *Journal of Medical Genetics*. **51** (3), 170–175 (2014).
11. Pesta, D., Gnaiger, E. High-resolution respirometry: OXPHOS protocols for human cells and permeabilized fibers from small biopsies of human muscle. *Methods in Molecular Biology (Clifton, N.J.)*. **810**, 25–58 (2012).
12. Horan, M. P., Pichaud, N., Ballard, J. W. O. Review: Quantifying mitochondrial dysfunction in complex diseases of aging. *Journals of Gerontology - Series A Biological Sciences and Medical Sciences*. **67 A** (10), 1022–1035 (2012).
13. Doerrier, C., Garcia-Souza, L. F., Krumschnabel, G., Wohlfarter, Y., Mészáros, A. T., Gnaiger, E. High-resolution fluorespirometry and oxphos protocols for human cells, permeabilized fibers from small biopsies of muscle, and isolated mitochondria. *Methods in Molecular Biology (Clifton, N.J.)*. **1782**, 31–70 (2018).
14. Zhang, J. et al. Measuring energy metabolism in cultured cells, including human pluripotent stem cells and differentiated cells. *Nature Protocols*. **7** (6), 1068–1085 (2012).
15. García-Roche, M., Casal, A., Carriquiry, M., Radi, R., Quijano, C., Cassina, A. Respiratory analysis of coupled mitochondria in cryopreserved liver biopsies. *Redox Biology*. **17** (March), 207–212 (2018).
16. Acin-Perez, R. et al. A novel approach to measure mitochondrial respiration in frozen biological samples. *The EMBO Journal*. **39** (13), 1–18 (2020).
17. SUITBrowserWeb. at <http://suitbrowser.oroboros.at/> (2021).
18. Cell metabolism assay kits, Seahorse assay kits and media. at <https://www.agilent.com/en/product/cell-analysis/real-time-cell-metabolic-analysis/xf-assay-kits-reagents-cell-assay-media> (2021).
19. Chance, B., Williams, G. R. A method for the localization of sites for oxidative phosphorylation. *Nature*. **176** (4475), 250–254 (1955).
20. Gnaiger, E. et al. Mitochondrial respiratory states and rates. *MitoFit Preprint Arch*. mitofit:190001.v6 (2019).
21. Gnaiger, E. Oroboros O2k-procedures: SOP O2k quality control 1: Polarographic oxygen sensors and accuracy of calibration Section Page. **03** (18), 1–21, at

1011 <http://wiki.oroboros.at/index.php/MiPNet06.03_POS-Calibration-SOP> (2020).
1012 22. Robinson, B. H., Petrova-Benedict, R., Buncic, J. R., Wallace, D. C. Nonviability of cells with
1013 oxidative defects in galactose medium: A screening test for affected patient fibroblasts.
1014 *Biochemical Medicine and Metabolic Biology*. **48** (2), 122–126 (1992).
1015 23. King, M. P., Attardi, G. Human cells lacking mtDNA: Repopulation with exogenous
1016 mitochondria by complementation. *Science*. **246** (4929), 500–503 (1989).
1017 24. Makrecka-Kuka, M., Krumschnabel, G., Gnaiger, E. High-resolution respirometry for
1018 simultaneous measurement of oxygen and hydrogen peroxide fluxes in permeabilized cells,
1019 tissue homogenate and isolated mitochondria. *Biomolecules*. **5** (3), 1319–1338 (2015).
1020 25. Fasching, M., Gnaiger, E. O2k quality control 2: Instrumental oxygen background
1021 correction and accuracy of oxygen flux. *Mitochondrial Physiology Network*. **14.06** (06), 1–14
1022 (2016).
1023 26. Gnaiger, E., Lassnig, B., Kuznetsov, A., Rieger, G., Margreiter, R. Excess capacity of
1024 cytochrome c oxidase. *Journal of Experimental Biology*. **1139**, 1129–1139 (1998).
1025 27. Gnaiger, E. et al. Mitochondria in the Cold. *Life in the Cold*. 431–442, Springer, Berlin,
1026 Heidelberg (2000).
1027 28. Fontana-Ayoub, Fasching, M., Gnaiger, E. Selected media and chemicals for respirometry
1028 with mitochondrial preparations. *Mitochondrial Physiology Network*. **02** (17), 1–9 (2014).
1029 29. Gerencser, A. A. et al. Quantitative microplate-based respirometry with correction for
1030 oxygen diffusion. *Analytical Chemistry*. **81** (16), 6868–6878 (2009).
1031 30. Krumschnabel, G., Eigentler, A., Fasching, M., Gnaiger, E. Use of safranin for the
1032 assessment of mitochondrial membrane potential by high-resolution respirometry and
1033 fluorometry. *Methods in Enzymology*. **542**, 163–181 (2014).
1034 31. Nászai, A., Terhes, E., Kaszaki, J., Boros, M., Juhász, L. Ca(2+)N it be measured? Detection
1035 of extramitochondrial calcium movement with high-resolution fluorespirometry. *Scientific*
1036 *Reports*. **9** (1), 1–13 (2019).
1037 32. Pajak, B. et al. 2-Deoxy-d-Glucose and its analogs: From diagnostic to therapeutic agents.
1038 *International Journal of Molecular Sciences*. **21** (1), 234 (2019).
1039 33. Mercier-Letondal, P., Marton, C., Godet, Y., Galaine, J. Validation of a method evaluating
1040 T cell metabolic potential in compliance with ICH Q2 (R1). *Journal of Translational Medicine*. **19**
1041 (1), 1–15 (2021).
1042 34. Sauerbeck, A. et al. Analysis of regional brain mitochondrial bioenergetics and
1043 susceptibility to mitochondrial inhibition utilizing a microplate based system. *Journal of*
1044 *Neuroscience Methods*. **198** (1), 36–43 (2011).
1045 35. Jackman, M. R., Willis, W. T. Characteristics of mitochondria isolated from type I and type
1046 IIb skeletal muscle. *American Journal of Physiology - Cell Physiology*. **270** (2 pt 1), c673–678
1047 (1996).
1048 36. Ponsot, E. et al. Mitochondrial tissue specificity of substrates utilization in rat cardiac and
1049 skeletal muscles. *Journal of Cellular Physiology*. **203** (3), 479–486 (2005).
1050 37. Schönfeld, P., Reiser, G. Why does brain metabolism not favor burning of fatty acids to
1051 provide energy-Reflections on disadvantages of the use of free fatty acids as fuel for brain.
1052 *Journal of Cerebral Blood Flow and Metabolism*. **33** (10), 1493–1499 (2013).
1053 38. Calderon-Dominguez, M., Mir, J. F., Fucho, R., Weber, M., Serra, D., Herrero, L. Fatty acid
1054 metabolism and the basis of brown adipose tissue function. *Adipocyte*. **5** (2), 98–118 (2016).

39. Divakaruni, A. S., Rogers, G. W., Murphy, A. N. Measuring mitochondrial function in permeabilized cells using the seahorse XF analyzer or a clark-type oxygen electrode. *Current Protocols in Toxicology*. **2014** (May), 25.2.1–25.2.16, (2014).
40. Iuso, A., Repp, B., Biagosch, C., Terrile, C., Prokisch, H. Assessing mitochondrial bioenergetics in isolated mitochondria from various mouse tissues using Seahorse XF96 analyzer. *Methods in Molecular Biology*. **1567**, 217–230 (2017).
41. Rogers, G. W. et al. High throughput microplate respiratory measurements using minimal quantities of isolated mitochondria. *PLoS ONE*. **6** (7), e21746 (2011).
42. Jordá, A., Zaragozá, R., Portolés, M., Báguena-Cervellera, R., Renau-Piqueras, J. Long-term high-protein diet induces biochemical and ultrastructural changes in rat liver mitochondria. *Archives of Biochemistry and Biophysics*. **265** (2), 241–248 (1988).
43. Jackson, C. B., Gallati, S., Schaller, A. QPCR-based mitochondrial DNA quantification: Influence of template DNA fragmentation on accuracy. *Biochemical and Biophysical Research Communications*. **423** (3), 441–447 (2012)
44. Hirsch, H.M. Tissue autoxidation inhibitors: II. The presence of inhibitor in intact cells; Assay of liver and hepatoma effect on radio-oxidations. *Cancer Research*. **16** (11), 1076–1082 (1956).
45. Picard, M. et al. Mitochondrial structure and function are disrupted by standard Isolation methods. *PLoS ONE*. **6** (3), 1–12, e18317 (2011).
46. Tanumihardja, E., Slaats, R. H., Van Der Meer, A. D., Passier, R., Olthuis, W., Van Den Berg, A. Measuring both pH and O2with a single On-Chip sensor in cultures of human pluripotent stem cell-derived cardiomyocytes to track induced changes in cellular metabolism. *ACS Sensors*. **6** (1), 267–274 (2021).
47. Harms, F., Stolker, R. J., Mik, E. Cutaneous respirometry as novel technique to monitor mitochondrial function: A feasibility study in healthy volunteers. *PLoS ONE*. **11** (7), 1–11, e159544 (2016).
48. Levitsky, Y. et al. Micro-respirometry of whole cells and isolated mitochondria. *RSC Advances*. **9** (57), 33257–33267 (2019).

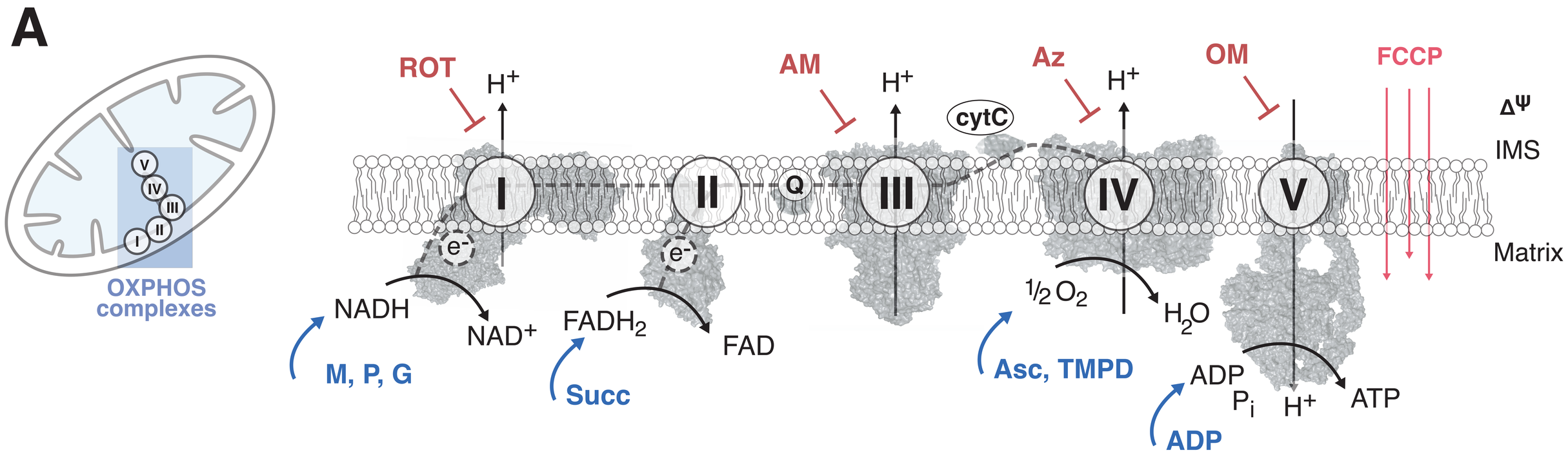

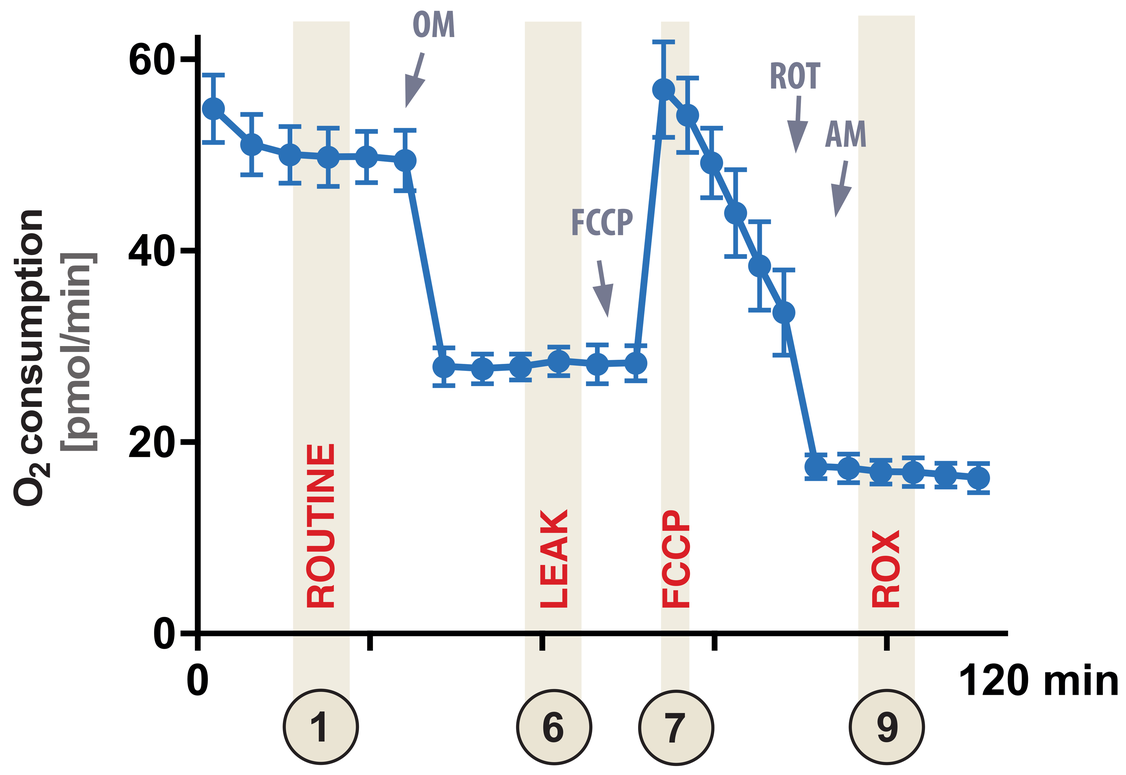

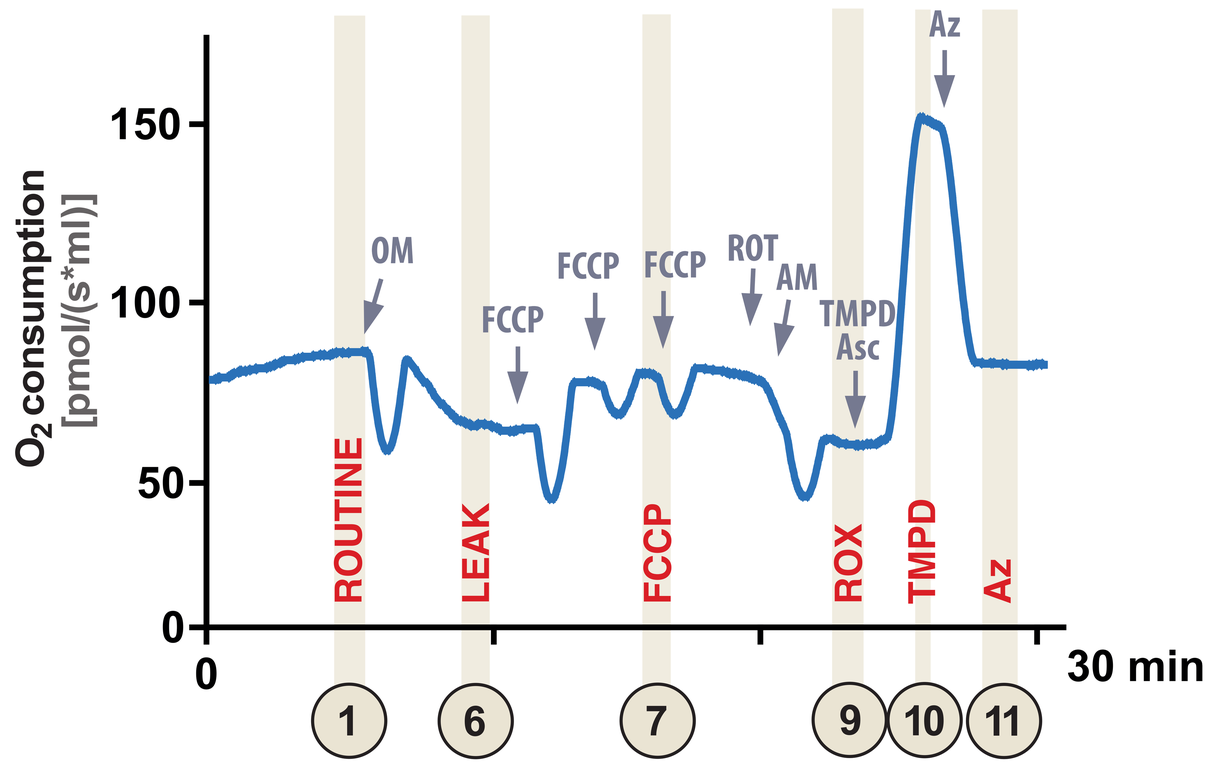

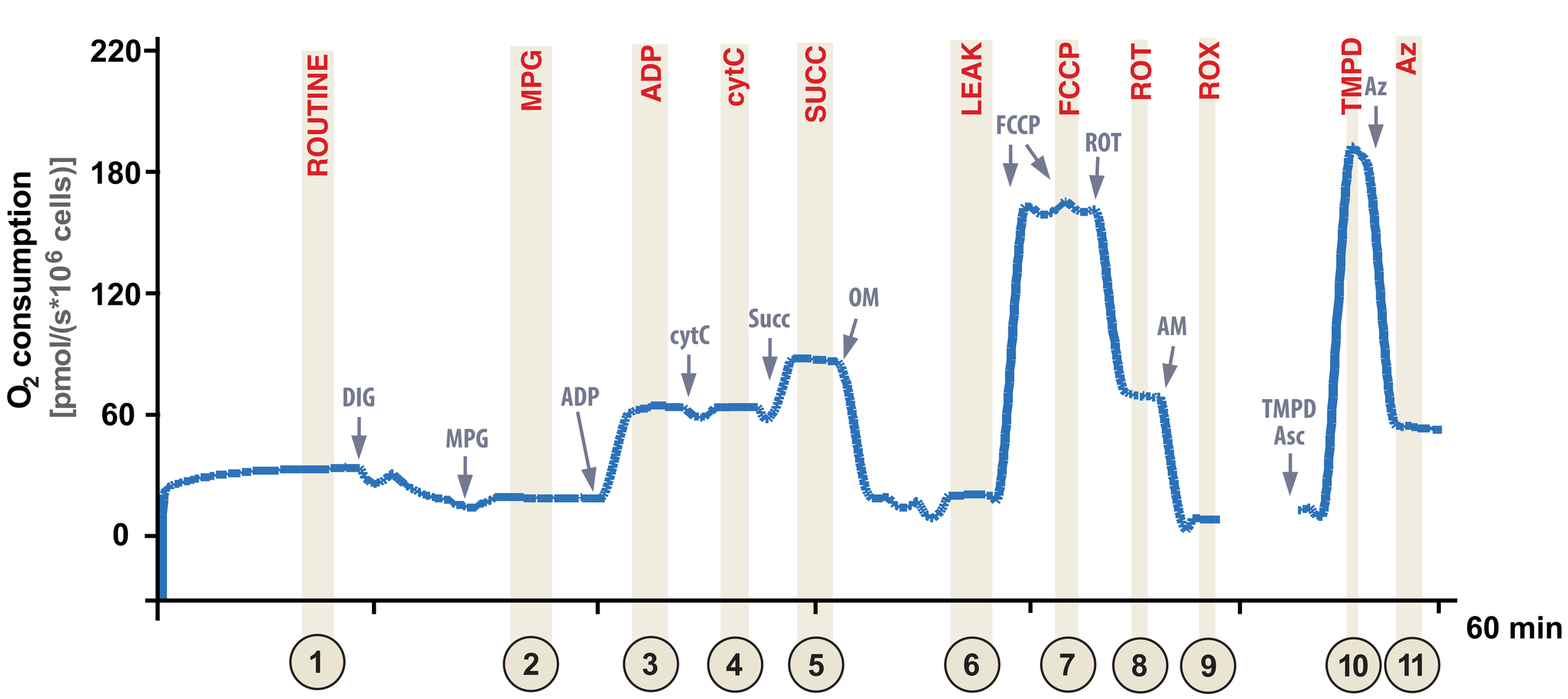

A Protocol outline

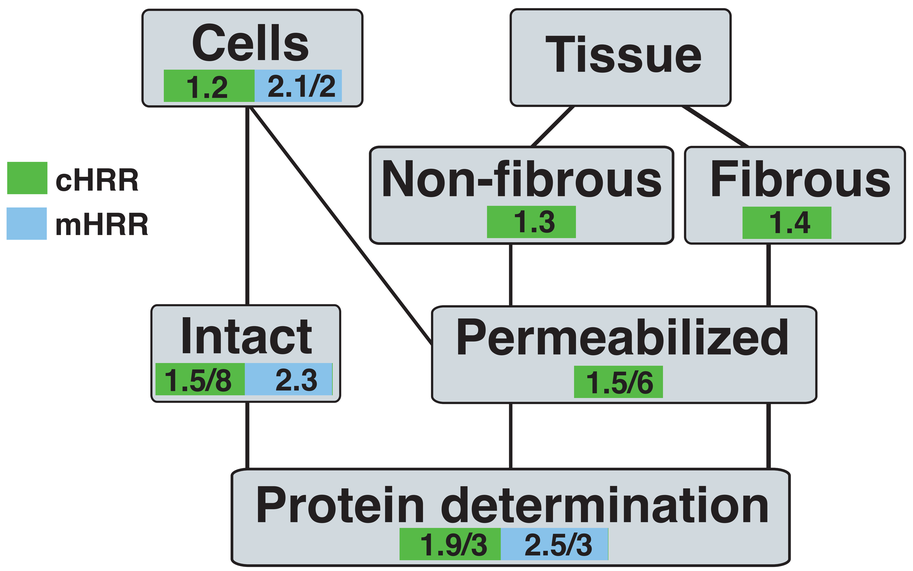

B cHRR

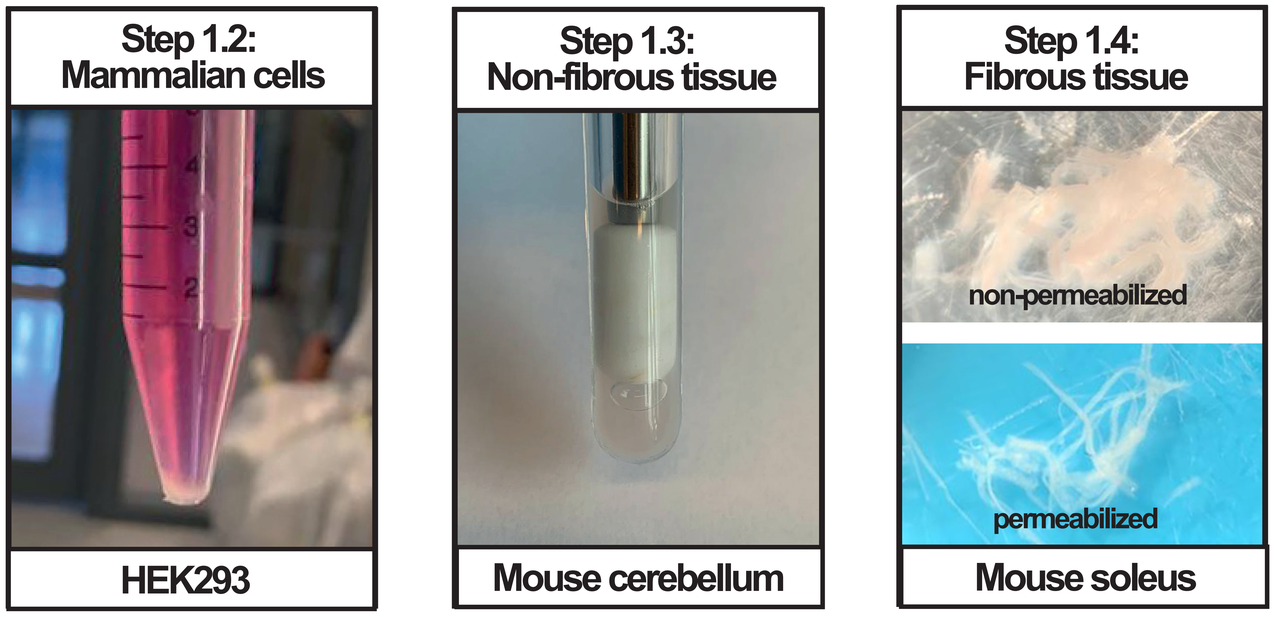

C Well confluency

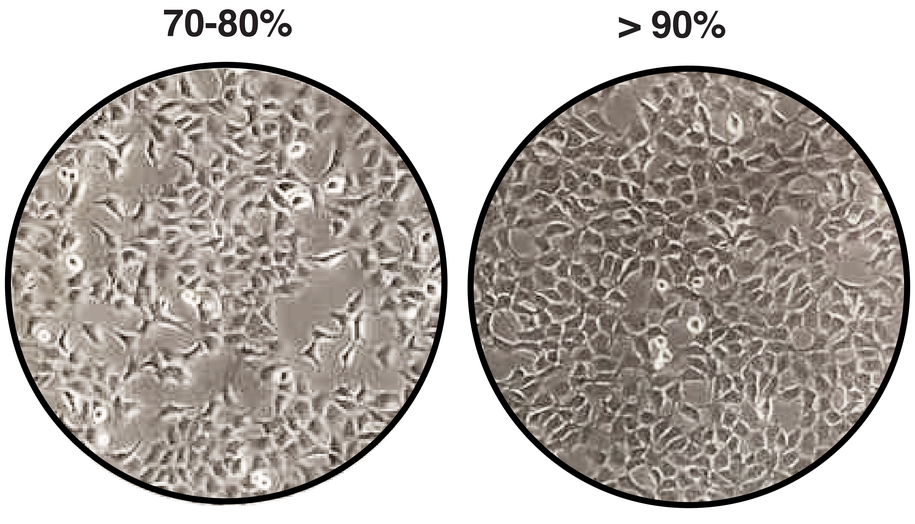

D mHRR Step 2.4: Standard

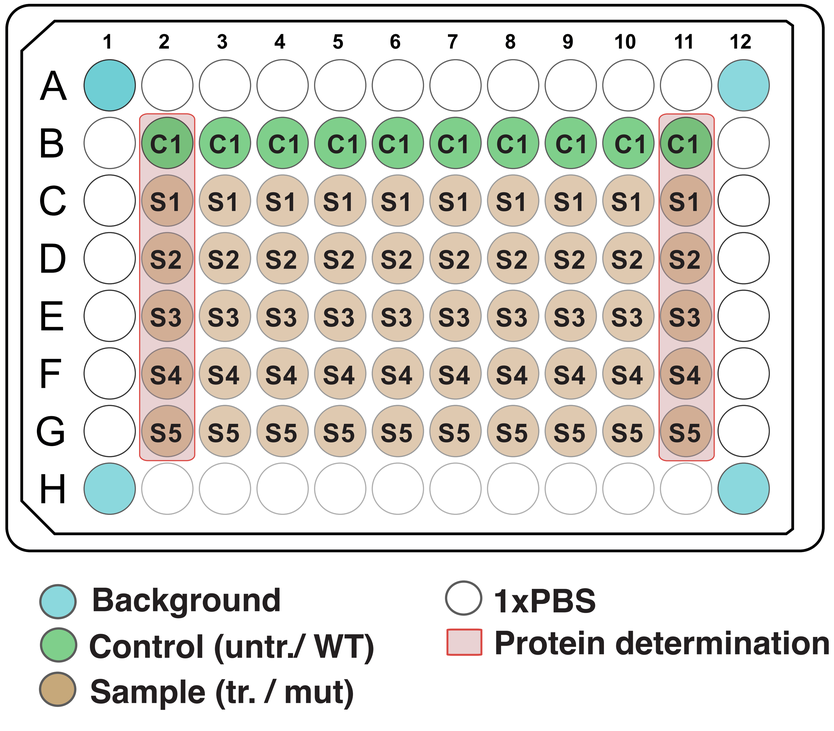

E mHRR Ports

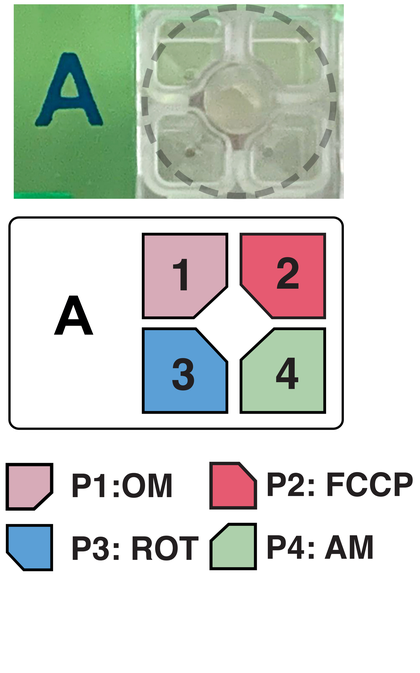

A

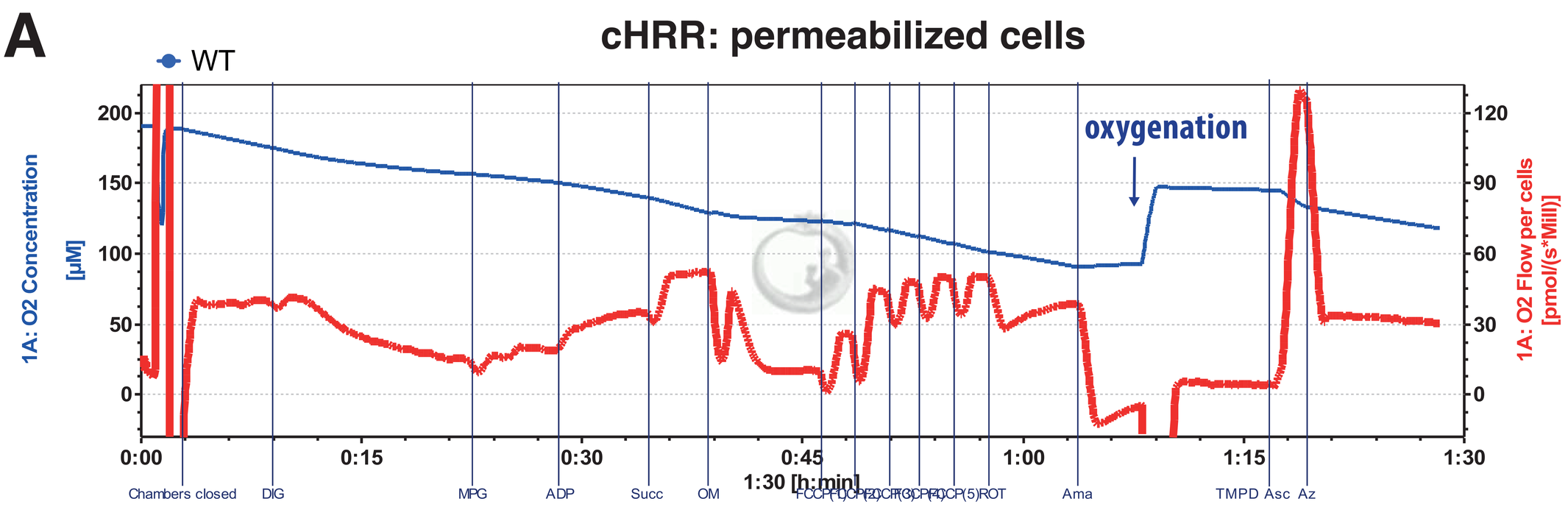

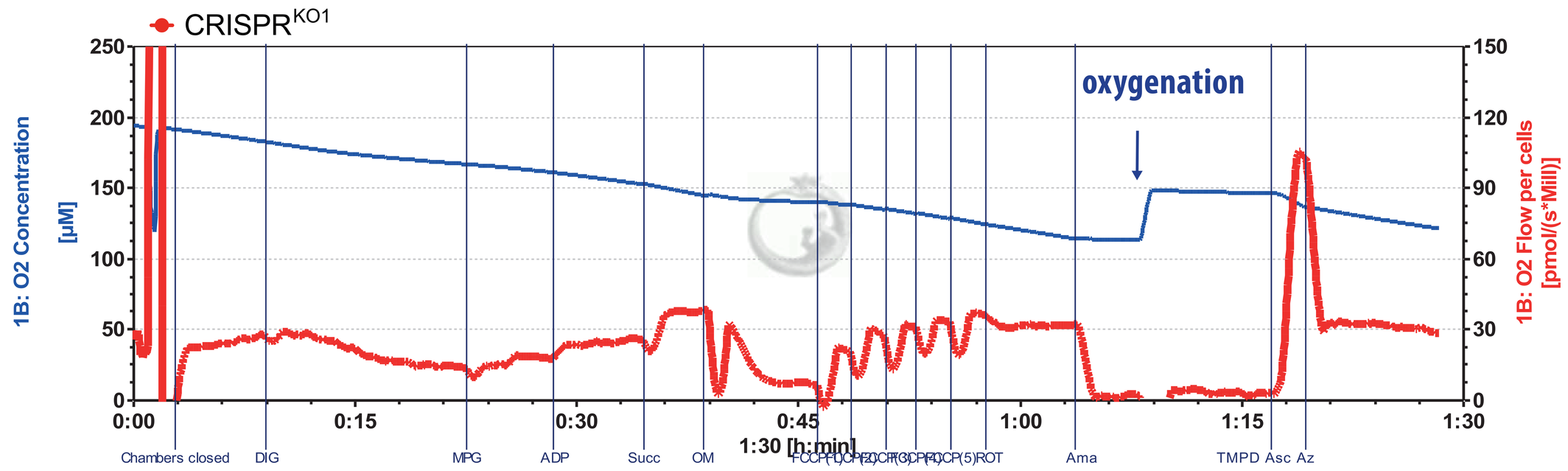

B

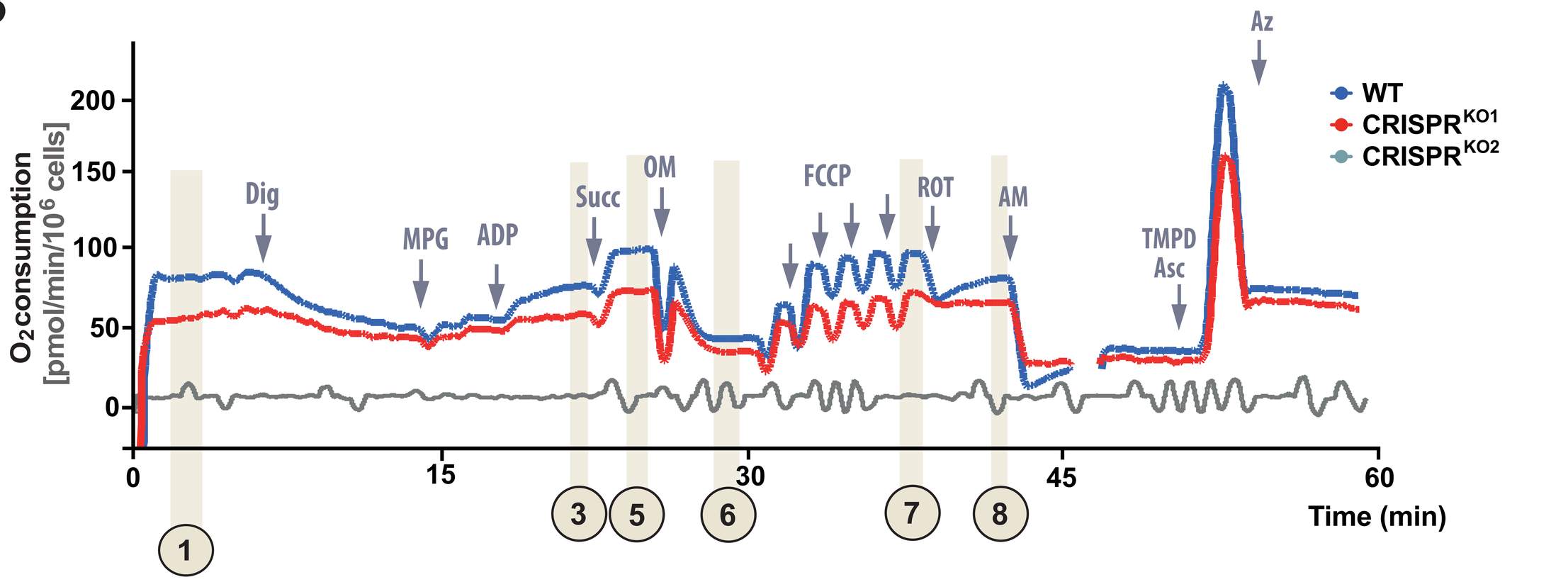

C

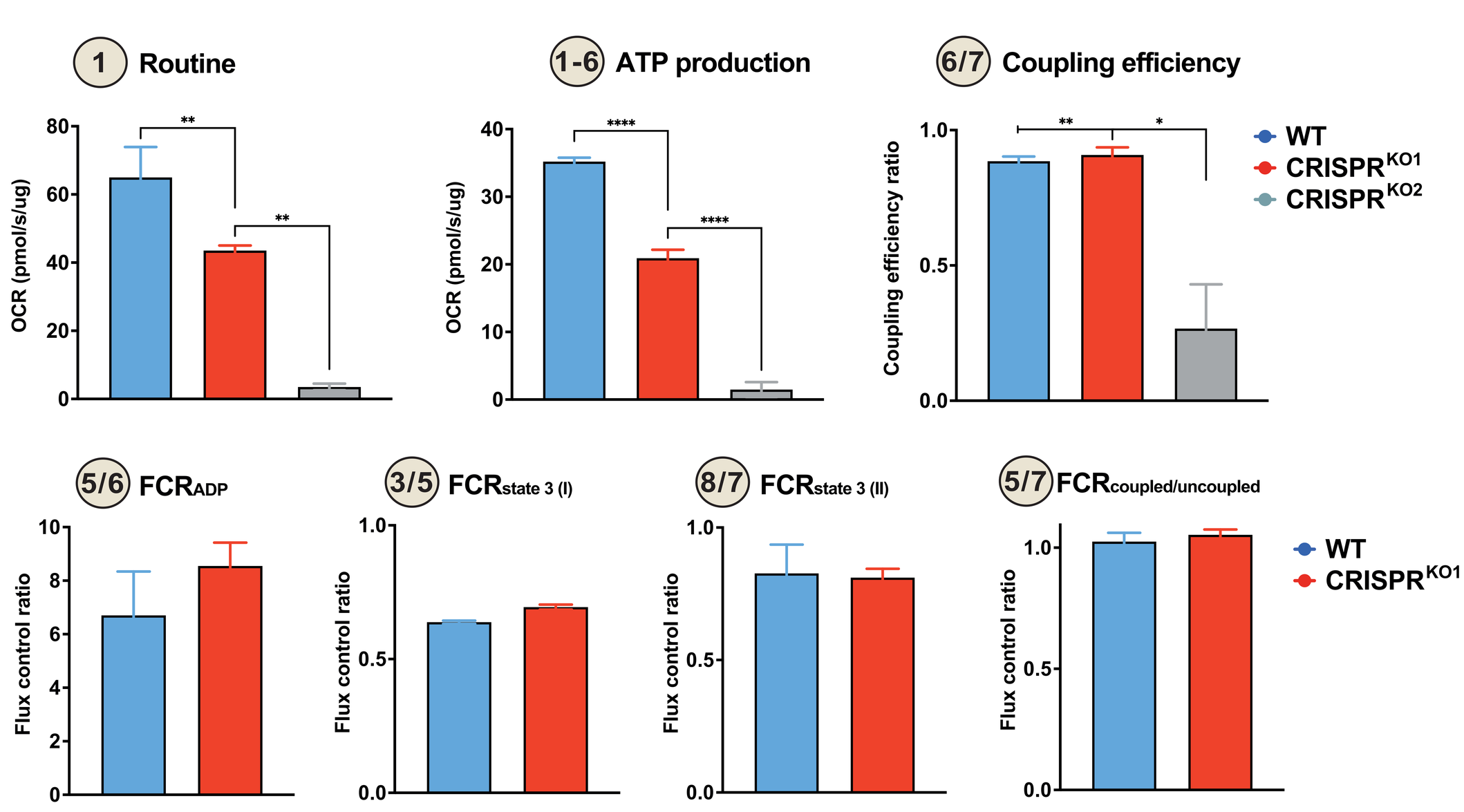

A

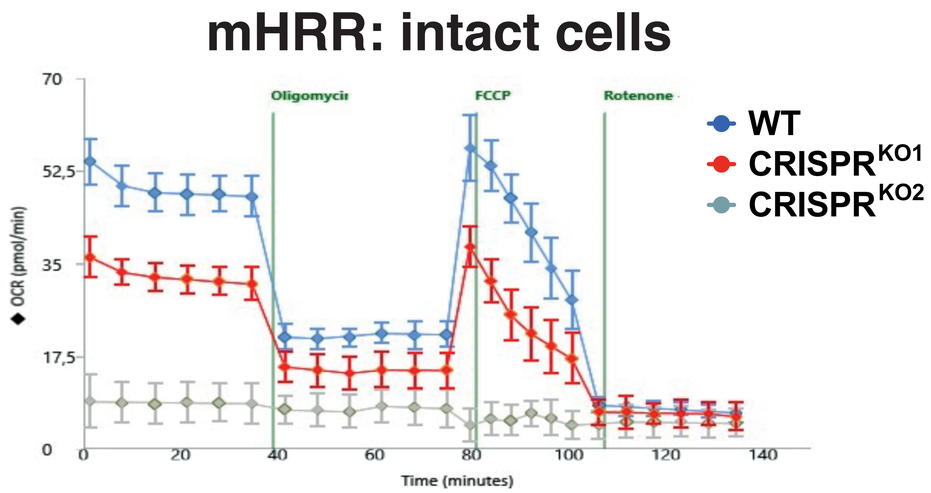

B

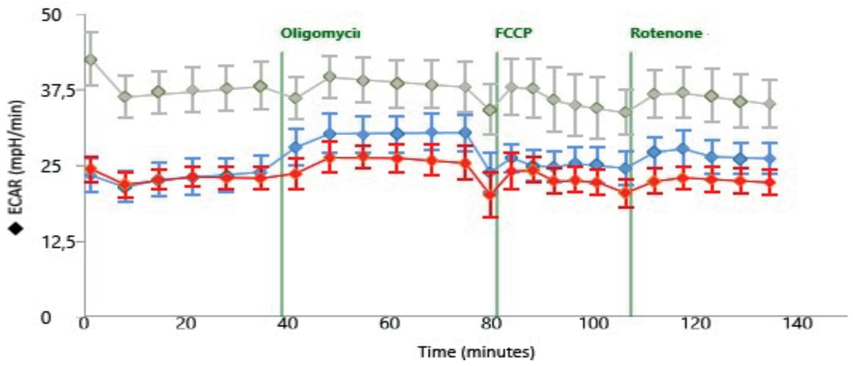

C

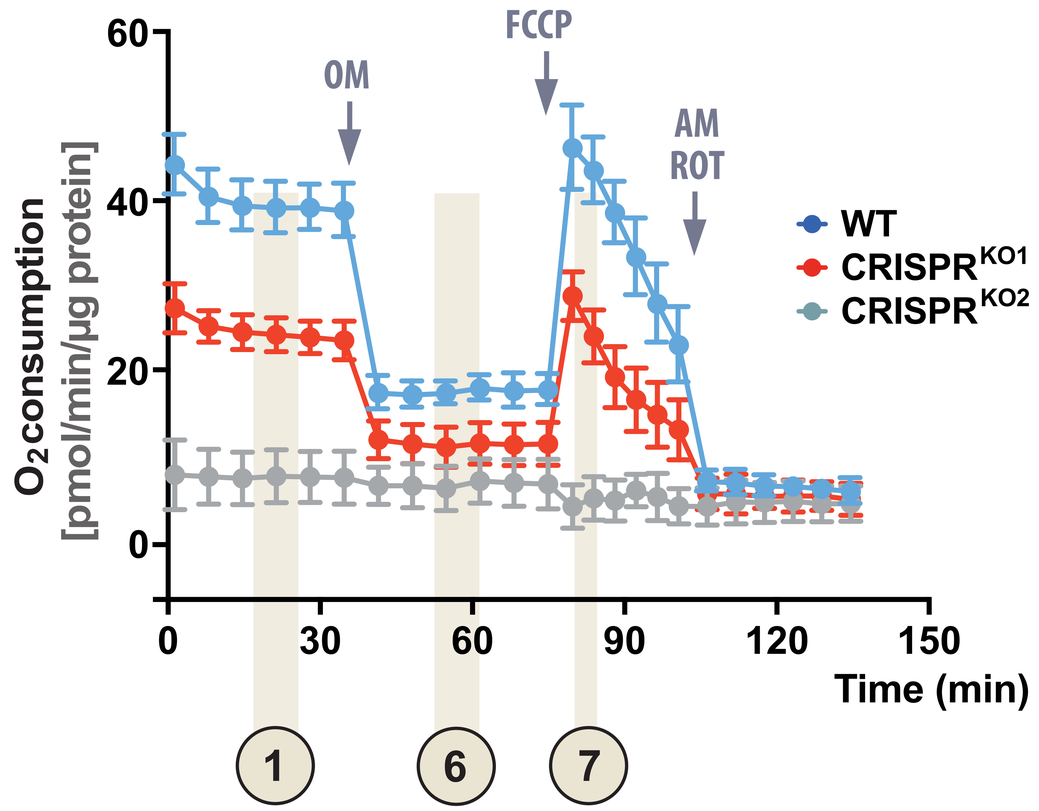

D

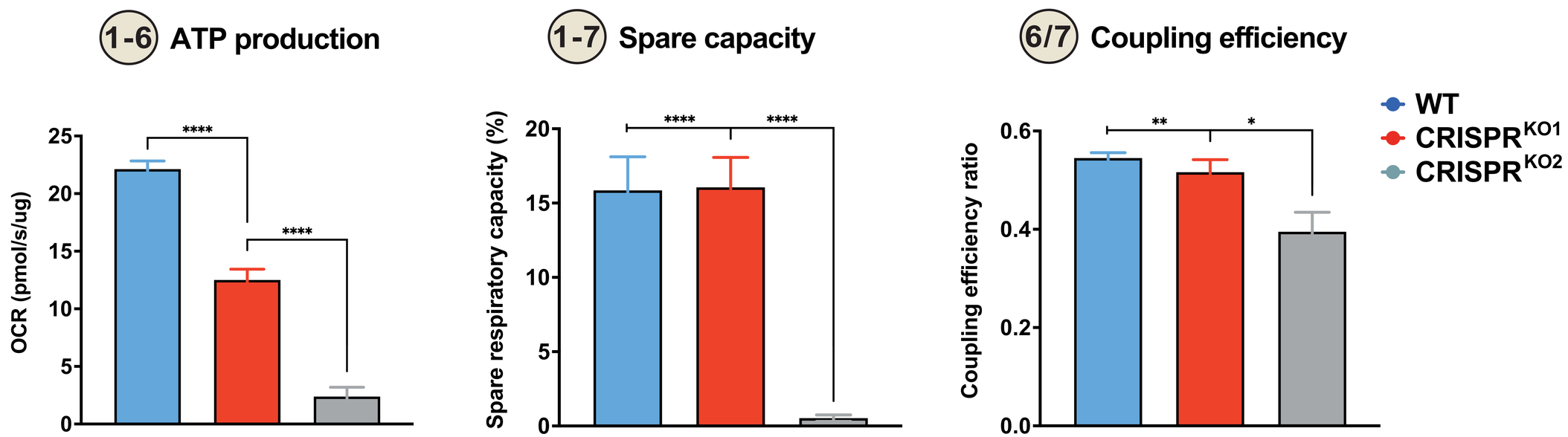

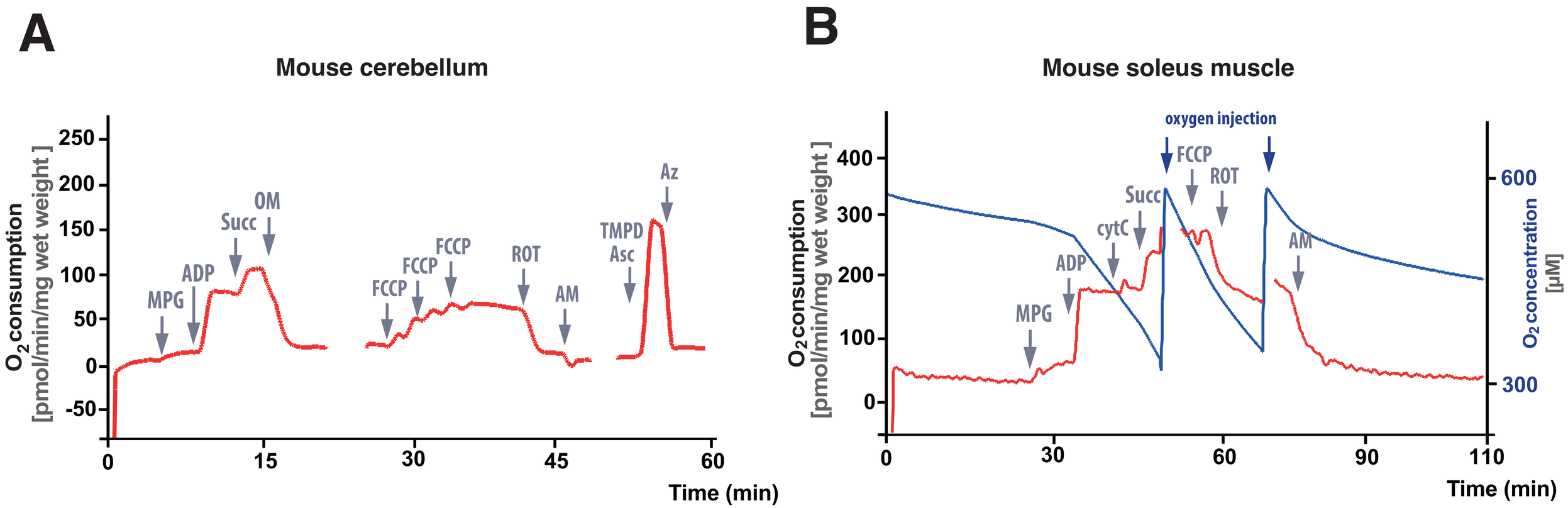

Table 1

Chemical	**Concentration**
BSA, fatty acid free	1 g/ L
D-sucrose	110 mM
EGTA	0.5 mM
HEPES	20 mM
KH_2PO4	10 mM
Lactobionic acid	60 mM
$MgCl_2 \cdot 6H_2O$	3 mM
Taurine	20 mM

Table 2

Chemical	Concentration
CaK2EGTA anhydrous	2.77 mM
Dithiothreitol (DTT)	0.5 mM
Imidazole	20 mM
K2EGTA, anhydrous	7.23 mM
MES hydrate	50 mM
MgCl2-6H2O	6.56 mM
Na2ATP	5.77 mM
Na2Phosphocreatine	15 mM
Taurine	20 mM

Dear Dr. Jackson,

Your manuscript JoVE63000R1 "High-resolution respirometry to assess bioenergetics in cells and tissues using chamber and plate-based respirometers" has been editorially reviewed and the following comments need to be addressed before your manuscript can be formally accepted.

Your revision is due by **Sep 17, 2021**.
Please make the changes/revisions in the attached manuscript file which has been formatted to fit the journal standard.

To submit a revision, go to the JoVE submission site and log in as an author. You will find your submission under the heading **Submission Needing Revision**.

Best,

Amit Krishnan, Ph.D.
Review Editor
JoVE
amit.krishnan@jove.com
617.674.1888
Follow us: Facebook | Twitter | LinkedIn
About JoVE

Dear Dr. Krishnan

Thank for your reply. We have adapted our protocol to the journals standard, addressed all comments within the manuscript (in green) and re-highlighted (yellow) the protocol for filming.

With kindest regards

Christopher Jackson

Ryan Awadhpersad